8-16-2017

Development of an In-situ Passive Sampling Device for Munitions Compounds and Sulfate

Joseph K Warren
joseph.k.warren@gmail.com

Development of an In-situ Passive Sampling Device for Munitions Compounds and Sulfate

Joseph Kyle Warren

B.S., University of Connecticut, 2012

A Thesis
Submitted in Partial Fulfillment of the
Requirements for the Degree of
Master of Science
At the
University of Connecticut
2017

2017

APPROVAL PAGE

Masters of Science Thesis

Development of an In-situ Passive Sampling Device for Munitions Compounds and Sulfate

Presented by

Joseph Kyle Warren, B.S.

Major Advisor_____

Penny Vlahos

Associate Advisor _____

Craig Tobias

Associate Advisor _____

Robert Mason

University of Connecticut 2017

Acknowledgements:

The completion and presentation of this master's thesis could not have been achieved without the help of several individuals across many different departments at Uconn and beyond!

First, I would like to thank my advisor, Dr. Penny Vlahos, for her guidance, support, and consultations on my research and development as a scientist. Without her mentoring me along the way, I still think I'd be trying to disassemble and rework lab equipment, rather than putting my research into writing.

Secondly, I would like to thank the two Uconn Marine Science faculty members that have mentored me throughout this process and served as my associate advisors. Dr. Craig Tobias, whose expertise in the field of underwater munitions compounds was invaluable, and Dr. Robert Mason, for always being willing to listen to whatever wastewater or analytical chemistry related tangent I had gone off on. I would like to thank both of them for being flexible in periods of frequent travel, and for several discussions that have helped give shape to what I would like to do in the future.

I would also like to thank David Cady and Amanda Dostie, for always being there during late nights and times where I had felt like temporarily giving up. You guys are my best friends and made this stressful time much more bearable. Your individual achievements drive me to want to be the best scientist I can be.

The faculty and support staff at Uconn Avery Point: Deb Schuler, Janet Laflamme, Patricia Evans, Gary Grenier, Veronica Rollinson, Elise Hayes, Dennis Arbige, and Todd Fake: thank you for always being willing to help, and mentor me in things that I lack knowledge on. Your expertise did not go unnoticed! I would especially like to mention Claudia Koerting here, as she trained and advised me on several analytical methods for chemical oceanography.

Vlahos lab mates: Allison Staniec, Rick Smith, Ellen Johnson, and Jessica Hinckley! You guys are the best! My time with you made the field work and lab time so much more enjoyable. I can't wait to hear what you guys will be achieving when you get done with school!

The Connecticut Center for Entrepreneurship and Innovation: Michelle Cote and Rae Asselin, I cannot thank you enough for the mentoring given during my time as an Accelerate Uconn member and Summer Fellowship fellow. You guys have given me a great business understanding and background, as well as funded the fellowship so that I could give CCEI my all! Thank you!

My collaborators at Washington University in St. Louis: Dr. David Fike and Jennifer Houghton. The sulfate project was a great success, and I can only attribute it to you guys making such a dynamic team. Thank you for bringing me out to St. Louis to work at your lab, and for giving me great insight into the biogeochemical sulfur cycle.

Finally, I would like to thank my parents, Allen and Denise Warren, for always driving me to do my best, and for never failing to support my endeavors, no matter how silly they may be. Without you, I would not be here today. I would also like to thank my little brother, Allen Kameron Warren: when I needed a break, you are always there for a hike or activity, and your disbelief of how much time scientists spend in a lab is still humorous to me. Without the three of you as my core support system, none of this would have been possible. I love you guys.

TABLE OF CONTENTS:

LIST OF FIGURES

Abstract:

Passive sampling is a novel method of analyte concentration from the environment that strives to bring greater ease to field sampling regimes than traditional liquid-solid phase extractions (SPE). It is easier to deploy than a Niskin bottle or CTD rosette, and easier to recover than hoisting up dozens of liters of water. Passive sampling also offers the opportunity for wider exploratory studies, as compounds can be selectively extracted back in lab, rather than having to select a particular phase SPE and follow phase-specific elution methods. In this study, Ethylene Vinyl Acetate copolymer (EVA) was used as a marine sorption and collection media. Its efficacy was tested in both ambient munitions sampling for TNT and RDX, and for sulfate in porewaters. For the munitions subset of samples, the interaction between salinity, temperature, and percent acetate composition of the EVA samplers was explored. It was found that salinity had a large increase on Log K_{EVA} from 0-5 PSU, then became nonlinear from 5-34 PSU. The initial increase was present for all EVA types, and the 5-34 PSU subset's Log K_{EVA} was affected in similar manner between EVA types. Increasing temperature was found to decrease munitions sorption over 5-25˚C, and it was found that EVA80 was the most efficient sorption media out of the EVA subtypes. This is likely due to dipole interactions from the increase in the polar acetate group. An EVA polymer seeded with barium containing organic compounds was tested for efficacy in sulfate precipitation to the film for use in isotopic sulfur measurements. Out of the many barium containing organic compounds selected for testing, barium oxalate was chosen for its efficiency at precipitating and trapping sulfate from the marine environment, while being able to be easily purified by an acid-catalyzed hydrolysis procedure. It was also proven that the EVA sampler does not add an isotopic bias through fractionation during precipitation to the film from the environment. Overall, it was proven that the Ethylene Vinyl Acetate copolymer is an effective passive sorption media for marine systems, for both munitions compounds and inorganic sulfate.

CHAPTER 1: Introduction

1.1 Passive sampling

Passive sampling is a method of analyte concentration utilizing a polymer based device to assess ambient pollutants in marine, soil, and atmospheric environments. Polymers are chosen that have a polarity favorable to sequestering target analytes, based on their octanol-water partition coefficients (Log K_{OW}s) or hydrophobicity. Laboratory experiments are used to determine the uptake kinetics of target contaminants in different environments (temperature, salinity, dissolved organic matter), and can thus be calibrated for an optimum exposure time, ensuring equilibrium between the thin-film sampler and the environment. Integrative, bulk samplers can also be used, and these differ by operating in the kinetic uptake phase, being able to sorb much larger amounts of contaminant than the thin-film (0.7 μm), equilibrium samplers.

Passive sampling has many benefits when compared to traditional sampling regimes. A traditional sampling method for a low Log K_{OW} contaminant would involve acquiring a several liter volume of water, passing the sample of water through a pre-treated separation column or cartridge utilizing a pump system, storing the cartridges without water or solvent in them, and then properly eluting the contaminants back in the lab. Passive sampling simplifies the field component of sampling. It allows for a much easier deployment, as you must place a small (5 cm x 5 cm) plate in an array at the proper depth for measurement, or near a point source of pollution, depending on the application. Recovery of the samplers is much simpler than a traditional extraction procedure, just pull them out of the water, dry them, and place into an air tight container kept at 4˚ C until extraction. Traditional extraction methods of soaking in solvent can be utilized, or, if the lab is equipped with it, a pressurized liquid extraction can be used for more efficient methods using less solvent.

These passive devices can be used as wide-scope, broad range contaminant samplers, or can be seeded as an admixture for compound-specific sampling devices. Sensors are another possible field of application for polymer based passive sampling devices, and compound specific sensors would be an ideal end goal of exploration.

1.2 Ethylene Vinyl Acetate

For this project, Ethylene Vinyl Acetate was selected as the polymer of choice. Ethylene vinyl acetate (EVA) is a copolymer made up of a ratio of non-polar ethylene groups to the polar vinyl-acetate group. This gives it an advantage for concentrating a wide range of contaminants

that can later be extracted selectively (St George et al. 2011). EVA has been studied as an ambient air sampler for PCBs, but in this study, we use EVA as an aquatic, and pore water concentrator for munitions and sulfate (Raub et al., 2015). The ratio of non-polar ethylene groups to the polar vinyl-acetate group can be adjusted in lab, resulting in admixtures that reveal the percent acetate nature of the polymer: EVA25, EVA40, and EVA80.

1.3 Munitions Project

One potential application for the Ethylene Vinyl Acetate passive sampler is for measuring contamination from unexploded ordinance (UXO) scuttled in marine environments. UXOs are a major problem around the world, with marine shelf deposition being the most cost-effective means of disposing. This results in point source pollution for TNT, RDX, chemical warfare agents (Sulfur mustard, arsenite, lewisite), and other munitions compounds. Over 1,900 sites have been identified for munitions contamination in North America alone, posing a threat to ecosystem health once the UXOs begin to leak.

This project explored the use of the EVA passive samplers as a device for measuring TNT and RDX in the environment. Through mesocosm setups ranging from one to twenty liters, and one field test, TNT, RDX, and their major derivative compounds were analyzed on a gas chromatograph fitted with an electron capture detector (GC-ECD). The uptake rate kinetics, and performance in varying temperature and salinity levels was ascertained, allowing for more accurate calibration based on ambient conditions. These results will lay the groundwork for future work done on trying to constrain the amount of munitions contamination in coastal systems.

For this project, the three main hypotheses explored were:

1. It is possible to passively sorb munitions compounds in both saline and freshwater systems, while constraining sorption kinetics.
2. Increasing salinity gradients will increase munition sorption
3. Decreasing temperature will increase munition sorption
4. Changing the percent acetate of the EVA film will increase the polarity of the film and may increase sorption of these relatively soluble organic compounds (TNT and RDX)

1.4 Isotopic Sulfate sampler

Sampling for inorganic compounds in the environment is a difficult task to accomplish. In a collaborative effort with Washington University in St. Louis, the EVA passive sampler was explored as a means for trapping sulfate in porewaters for isotopic measurements. This effort involved exploring several different barium containing organic compounds in which to seed within the EVA polymer. After many tests of uptake efficiency and extraction protocol, barium oxalate was chosen, as it was able to sequester sulfate from the environment efficiently and can be removed through an acid catalyzed hydrolysis reaction while leaving the target compound, barium sulfate, behind for isotopic analysis by Elemental Analysis/Isotope Ratio Mass Spectrometry (EA/IRMS).

For this project, efforts at Uconn revolved around testing the various barium containing organic compounds for seeding, then quantifying and constraining bulk uptake of sulfate, and improving extraction efficiency and percent yield of barium sulfate from the mass of insoluble inorganics removed from the sampler coating. The collaborators at Washington University analyzed for compound purity and isotope values on the EA/IRMS, ran the secondary ion mass spectrometer (SIMS), and measured hydrogen sulfide, another important player in the biogeochemical sulfur cycle, via μ-sense probe. The two teams came together twice during this project: once for a preliminary field test in Sippiwissett salt marsh in Cape Cod, MA, and a second time for extraction efficiency tests in St. Louis.

It was found that by utilizing an acid-catalyzed hydrolysis reaction for removal of excess barium oxalate, extraction efficiencies could be, on average, 75%. Through lab tests at Washington University, it was confirmed that adding the acid does not significantly alter the isotopic signal of the barium sulfate trapped in the film, nor does hydrogen sulfide get trapped and oxidized to sulfate within the film or extraction process.

The hypotheses addressed in this part of the project include:

1. Sulfate ions from bulk solutions will diffuse into the EVA film
2. It is possible to seed the EVA polymer with Barium containing organic compounds,
3. Ions diffusing into the film will preferentially bind with barium ions introduced through organic barium compounds
4. That precipitated barium sulfate can be extracted from the bulk film
5. The spatial resolution of the barium containing EVA Sampler will be resolved enough for in-situ sulfate mapping

6. The film will capture sulfate for subsequent isotopic sulfur measurement without introducing an isotopic bias.

The work from this study has been published in ACS Earth and Space Chemistry (DOI: 10.1021/acsearthspacechem.7b00012) on 11 April, 2017.

CHAPTER 2. Passive Sampling of Munitions Compounds in Marine Systems

Joseph K. Warren[1*], Penny Vlahos[1], Richard Smith[2], Craig Tobias[1],

[1]*University of Connecticut, Department of Marine Sciences*

1080 Shennecossett Road, Groton, CT 06340

[2] *Global Aquatic Research LLC, 6276 Ridge Rd., Sodus, NY 14551*

*Corresponding Author Tel.: 860-878-8145

Email Address: Joseph.k.warren@gmail.com (Joseph K. Warren)

Abstract:

Over the last century, Unexploded ordnances (UXOs) have been deposited in marine shelf systems for lack of cost effective alternatives. Underwater UXOs have the potential to leak TNT and RDX, commonly used chemical munitions, and contaminate local waters, biota, and sediments. The rate at which this contamination occurs in the environment is relatively unknown, and the cost- and time-prohibitive nature of sampling across sites makes mapping difficult. Here we assess the efficacy of ethylene-vinyl acetate (EVA) for sampling relatively soluble munitions compounds over a range of environmental conditions (i.e. changes in temperature and salinity), and optimize the composition of the passive sampling polymer. The EVA sampler was able to successfully detect ambient concentrations of lingering munitions compounds from field sites containing UXOs. The sampler affinity for the munitions in terms of an EVA-water partition coefficient was greater than the standard octanol water values for each target compound. Partitioning over the natural ranges of salinity did not change significantly though uptake varied consistently and predictably with temperature. Increasing the vinyl acetate to ethylene ratio of the polymer corresponded to an increase in uptake capacity, which supports a dipole-dipole interaction mechanism between the munitions and the polymer. This sampler provides a cost effective means to map and track leakage of UXOs both spatially and temporally.

Introduction:

Since World War I, the production, testing and use of highly energetic explosive compounds has left behind a legacy of contamination worldwide. Munitions such as 2,4,6-trinitrotoluene (TNT), 1,3,5-trinitro-1,3,5-triazine (RDX), high melting explosives (HMX: a byproduct of RDX production), picric acid, and nitro-benzene have been used frequently in military and naval warfare. In the United States alone, over 1,900 sites have been identified as having explosive material contamination that has persisted from the turn of the 20th century (Kalderis et al.2011). In Europe and North America, unregulated dumping of munitions into seawater (frequently coastal systems) was a common practice throughout most of the 20th century. This results in the leaching of munitions into the sediment and water columns of surrounding sites, including fishing grounds, exhibiting appreciable concentration of parent and degradation compounds (Kalderis et al. 2011).Aside from the threat of un-exploded ordnances (UXOs) left behind from vacated missions, legacy contamination from wastewater used in production of these compounds, and the cleaning of equipment used to produce them, has resulted in a global issue that needs serious attention.

TNT and RDX introduced into marine systems poses a number of environmental and human health concerns. Both compounds have significant bio-concentration factors in commercially harvested bivalves, fish and crustaceans (Ballentine et al. 2014), particularly in egg sacks, as well as marine bacteria (Drzyzga et al. 1995). The parent munitions and their degradation products have been shown to be hazardous to humans through pathways such as inhalation, ingestion, and absorption. Acute exposure to these compounds can result in dermatitis and jaundice, with higher-level exposures leading to hepatic failure and cyanosis (Yinon 1990).

Both RDX and TNT are subject to transformation (the production of organic derivatives), partitioning onto sediments and suspended particulate matter (SPM), and mineralization to C and N containing inorganic compounds (Smith et al. 2013, 2015a, b, Ariyarathna et al. 2016). Composition of the soil in terms of particle size and organic matter concentration also has a direct effect on the reactivity of the munitions in the environment (Phillips et al. 2004). The relative extent of these various pathways, as well as the type of derivatives produced during transformation, will play a determining role in their persistence, toxicity, and bioconcentration in marine systems. However, despite the constraints on several of these processes in marine mesocosms and flask experiments, few studies exist for tracking the actual fate of these

compounds in the ocean. One of the challenges associated with this is limitations with sampling resolution in marine systems.

One potential method for overcoming this limitation is passive sampling. The passive sampler used in this study is based on ethylene vinyl-acetate (EVA) (**Figure 1**), which is a thermoplastic that has both hydrophobic and hydrophilic components (St. George et al. 2011, Raub et al. 2015, Vlahos et al. 2017). EVA has unique properties that can be targeted based on the percent acetate (by weight) composition. The polarity of the EVA increases proportionally with the number of acetate units present in the polymer, which is useful for developing compound specific samplers, or for selectively sorbing target compounds at varying salinities. The physical properties of the polymer also change and are summarized in **Table 1**. These include hardness, clarity (opacity) and elasticity. Mixtures lower than 80% acetate by weight are thermoplastics, while the 80% mixture contains kaolin, poly(vinyl-alcohol), talc and quartz and is marketed as an admixture for latex dispersion. EVA40 (40% vinyl acetate by weight) has been used previously for persistent organic pollutants including pesticides as well as polychlorinated bi-phenols (Raub et al. 2015, St George et al. 2011, Tucca et al. 2014). The low cost, low toxicity, and robust film coating of ethylene vinyl-acetate based samplers makes them ideal for both localized and broad scale sediment, water or atmospheric sampling.

To our knowledge, passive sampler technology has not been comprehensively utilized for a broad range of munitions compounds in aquatic settings though some preliminary studies have shown promise (Rosen, 2015). Here, we investigate the application of EVA for passive sampling of relatively soluble, nitroso- and aromatic, nitrogen containing munitions. Thin-film EVA samplers were exposed to TNT and RDX in various simulated environments to optimize and calibrate the sampling device for application in real aquatic environments. Finally, the samplers were deployed in two field sites containing UXOs to ascertain their performance under field conditions.

Figure 1: Structure of EVA. Note: the n and m define the average number of ethyl and acetate groups respectively for a given EVA type.

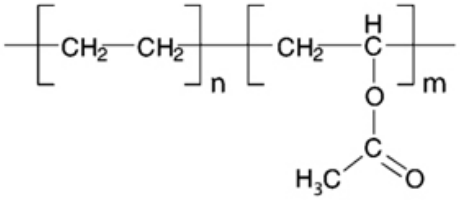

Table 1: Properties of the different % Acetate EVAs. Here n and m refer to the number of ethyl and acetate groups per average EVA unit respectively.

% Vinyl acetate	n	m	Polarity ratio	MW per unit $gmol^{-1}$	Density gml^{-1}	Elasticity	Opaqueness	Melt Temp ˚C
25	9	1	1:10	338	0.948	Hard	White	75
40	9	2	2:11	424	0.986	Malleable	Clear	60
80	3	4	4:07	428	NA	Powder	NA	NA

Materials and Methods

Chemicals. Ethylene Vinyl-Acetate pellets were sourced from Sigma Aldritch (EVA 40%, 25% Acetate by weight) and Polysci (EVA 80%). Methylene chloride (DCM) acetonitrile and methanol UHP were purchased from Fisher Optima. The samplers and water samples collected in this experiment were analyzed for TNT, RDX, and their respective breakdown products: 2A-DNT, 4A-DNT, hexahydro-1,3,5-trinitroso-1,3,5-triazine (TNX), hexahydro-5-nitro-1,3-dinitroso-1,3,5-triazine (DNX), and hexahydro-3,5-dinitro-1-nitroso-1,3,5-triazine (MNX). 3,4-DNT was used as an extraction standard as it is normally a non-naturally occurring compound and is not produced from the breakdown of munitions compounds. Standards were purchased from Accustandard (3,4-DNT, 2A-DNT, 4A-DNT), SRI International (MNX, DNX, TNX, courtesy of Dr. Ronald Spangord), and China Lake NAWCWD (TNT and RDX, Courtesy of Dr. Stephen Fallis).

Coating and Preparation of Thin-Film EVA Samplers. Two grams of EVA pellets were dissolved per 100 milliliters of DCM, covered and stirred for two to four hours (St. George et al. 2010) or until full dissolution, based on the percent acetate of the polymer. Substrates of stainless steel, as well as titanium, were used in this experiment, with dimensions of 5.0 x 7.5 cm. The 'plates' were combusted at 450˚C, rinsed with acetone, and coated by dipping into the well-mixed DCM/EVA mixture and allowing time for the solvent to evaporate. This was repeated for a total of three times to get a uniform coating with a film thickness of about 7 μm. After preparation, samplers were wrapped in foil, placed into an airtight plastic bag, and refrigerated at 4˚C to minimize contamination. Before exposure, these refrigerated plates were kept in their bags until reaching ambient room temperature.

Preparation of Integrative (Bulk) EVA Samplers. Utilizing the same raw materials as outlined above, integrative, bulk contaminant, samplers were also prepared for field deployment. Two grams of EVA pellets are dissolved into 50 milileters of DCM in a small, sealed vial over several hours, then poured into a 'well' like device where the film can form as the methylene chloride evaporates. Gentle heat (27-30˚C) was used to ensure uniform evaporation and film coating. After preparation, the thicker filmed samplers were wrapped in foil, placed into airtight plastic bags, and refridgerated to minimize contamination.

Extracting Thin-Film EVA Samplers. The exposed samplers were dried (<10 min) under the flow of ambient air in a fume hood, placed into jars with ~200 ml methanol (St. George et al. 2009), and allowed to soak for 24 hours. The solvent was collected into a round bottom flask and another 200 ml aliquot of methanol was added to the jar for a second 24 hour extraction. Both extracts were combined, spiked with an extraction standard of 3,4-dinitrotolule, and concentrated via rotary evaporator (Buchi Rotovapor-R215) to ~ 5 ml, and 15 ml acetonitrile was added to the residual for solvent exchange. Rotary evaporation was carried out until only 5 ml of acetonitrile remained. Extracts were then transferred to snub-nosed vials, while the round bottom flasks were rinsed with another 1-2 ml acetonitrile, and the collected fractions evaporated under a gentle stream of nitrogen to 1 ml. The sample was immediately analyzed or refrigerated at 4˚ C until analysis.

Extracting Integrative EVA Samplers. A small subset of integrative samplers were extracted using pressurized liquid extraction (PLE) methods utilizing a Fluid-Management Systems PLE. The integrative films were removed from their carriers, and placed into a 100-ml reaction vessel, and the head space was reduced by addition of Ottawa Sand (Fisher). The vessel was flushed and filled with methanol, then held at 1500 psi, and 50˚C for ten minutes while extraction took place. The extraction was repeated a second time. The methanol extract (~500 ml) was collected into a round bottom flask, reduced to < 2 ml and transferred to a GC vial utilizing the rotary evaporation and sample transfer methods outlined above. Based on ratios of measured to expected sample peaks of the internal standard 3,4-DNT, extraction efficiencies were 68% and 76% on average for TNT and RDX, respectively.

Water Sampling. Concentrations of TNT and RDX in the water column were carried out using salting out procedures outlined by Miyares & Jenkins (1990) and modified by Ballentine et al. (2015). A 4 ml sample of water was placed into a 15 ml centrifuge tube preloaded with 1.5g sodium chloride (combusted, FisherSci) and 1.5 ml of acetonirile. The tubes were shaken, sonicated for ~10 minutes, and allowed to settle before the acetonitrile fraction was collected. A second extraction was performed with 1 ml of acetontrile, following the sonication and settling method as before. The two extracts were combined, and the solvent was concentrated under a gentle stream of nitrogen to final volume of 1ml before transferring to a GC vial prior to analysis.

Loading Experiment Setup. For the initial loading experiments, a 15L glass tank was filled with 10L of either milli-q or sand filtered seawater from Long-Island Sound (salinity of 34). TNT and RDX were added to the tank for a target initial concentration of 1 mg/L (1µg/ml). After 1 hour of equilibration time, racks were placed into the tank to allow for full exposure to the water column. For the uptake regime of the experiment, all 22 plates (12 time points with duplicates, 24 plates total, 2 blanks) were placed into the same closed-system, munitions (TNT & RDX) spiked tank. Duplicate samplers were removed at set time points (0.5, 1, 2, 6, 24 h), with the remaining twelve samplers allowed to equilibrate for another 24 h before the depuration regime (48 h).

Equilibrium Partitioning as a function of Temperature & Differing EVA Types. For the varying percent acetate EVA experiment, samplers of each EVA25, EVA40, and EVA80 were coated in triplicate, and placed into 250mL glass jars containing TNT and RDX in milli-q. Blanks were produced using the same coating protocol as before, and placed immediately into non-spiked solution when the experiment started. After six hours of exposure, the samplers were removed, and allowed to dry in a fume hood. Extraction procedures were followed as outlined above. This experiment was reproduced at 25, 14, and 4 ˚ Celsius.

Instrumentation. Analysis was carried out on an Agilent 7890A gas chromatography/electron capture detector (GC/ECD). The method was originally described by Pan et al. (2005), with modifications by Smith et al. (2013) and Ballentine et al. (2015). A 1 microliter aliquot of

solution was injected in pulsed/splitless mode into a double taper pulsed/splitless liner. Helium (Airgas, UHP HE300) was used as a carrier gas at a flow rate of 11.9 ml min^{-1} through a HP-DB5 column (30m x 320 μm, 0.25 μm, Agilent). The initial oven temperature was set to 90˚C, with two ramps over the course of 14 minutes. Ramp one was 10 ˚C/min starting at 90˚C, and held for 1.5 minutes once reaching 200˚C. Ramp two was 3.5 ˚C/min to 250˚C, and was held for 1.9 minutes. Peak areas were converted to compound concentrations with an external concentration curve containing TNT, RDX, 2A-DNT, 4A-DNT, 3,4-DNT, TNX, DNX, and MNX. The reporting limit for all compounds was 0.7 ng ml^{-1}.

RESULTS AND DISCUSSION:

TNT/RDX Uptake Experiment. Results from uptake experiments in both fresh and saline systems are summarized in **Table 2**. In all cases, there is rapid uptake by the sampler over the first two hours of the experiment for both TNT **(Figure 2A)**, and RDX **(Figure 2B)**. Initial uptake rate constants were $k_1 = 0.286\ h^{-1}$ for TNT in milli-Q solution and $k_1 = 0.271\ h^{-1}$ in 34 gkg^{-1} seawater. RDX in milli-q and saline water treatments had values of $k_1 = 0.140\ h^{-1}$, and $k_1 = 0.190\ h^{-1}$ respectively. Steady state was reached between 5-6 h for both compounds. At 6 h the dimensionless log $K_{EVA/W}$ values were 2.14 and 2.04 for TNT and 1.44 and 1.34 for RDX in Milli-Q and saltwater solutions respectively. The offloading rates (k_2) in **Table 2** were calculated assuming equilibrium using $K_{EVA-W} = k_1\ k_2^{-1}$. Note in **Table 2** the estimated offloading rates are not appreciably different between fresh and saltwater systems. The slower offloading in saltwater is expected due to the lower solubilities of TNT and RDX in saline systems. Based on the parmeters in this experimental design the sampling rates of the samplers were 430.5 and 79.06 L/hr for TNT and RDX in freshwater and 329.4 and 4.878 L/hr for TNT and RDX saltwater respectively.

Table 2: Summary of uptake and depuration rates for TNT and RDX at 24 ^{o}C for different water types spiked to 0.05 mg L^{-1} of munition (using EVA40).
Note: $K_{EVA-W} = k_1 k_2^{-1}$

	TNT			RDX		
	Milli-Q (0 gkg^{-1})	Artificial Seawater (30 gkg^{-1})	Actual Seawater (34 gkg^{-1})	Milli-Q (0 gkg^{-1})	Artificial Seawater (30 gkg^{-1})	Actual Seawater (34 gkg^{-1})
k_1 (h^{-1})	0.286 (+/- 0.002)	NA	0.271 (+/- 0.002)	0.140 (+/- 0.010)	NA	0.190 (+/- 0.043)
k_2 (h^{-1})	0.002 (+/- 0.003)	NA	0.002 (+/- 0.001)	0.005 (+/- 0.010)	NA	0.009 (+/- 0.043)
$logK_{EVA-W}$	2.14	2.10	2.04	1.44	1.55	1.34

***Figure 2 A**: Uptake curve for TNT Milli-Q vs Seawater for 40% Acetate EVA*

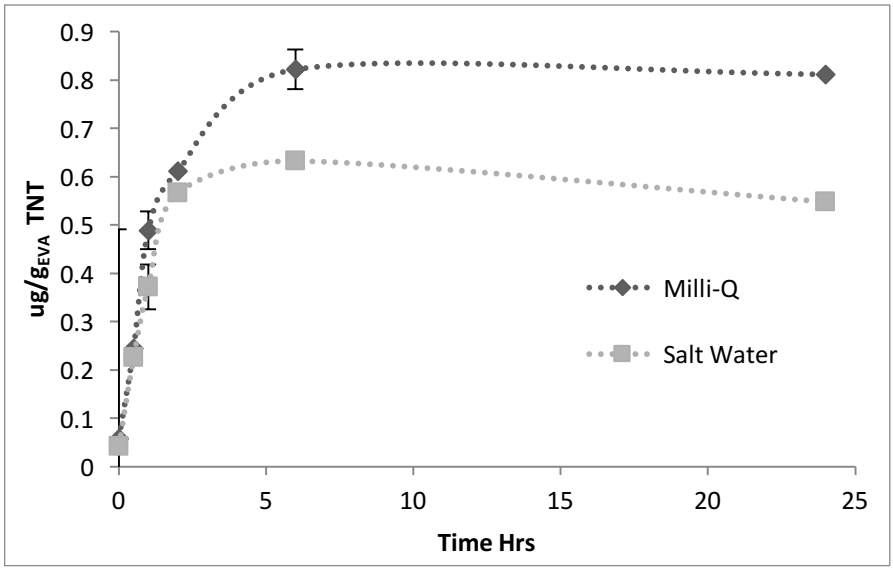

***Figure 2 B:** Uptake curve for RDX: Milli-Q vs Seawater for 40% Acetate EVA*

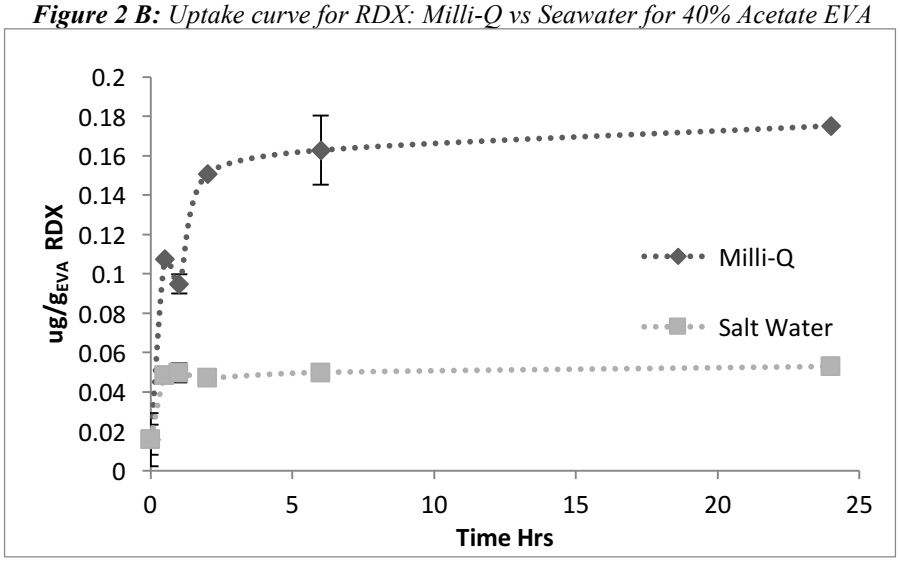

Uptake of EVA types. Table 3 summarizes the partitioning of TNT and RDX onto EVA films of varying polarity. EVA 20, 40 and 80 represent the percent vinyl acetate by mass in each film where EVA20 is the least substituted and therefore the least polar of the films and EVA80 is the most. The influence of salinity and temperature was investigated for all three film types to evaluate consistencies or inconsistencies in film responses to these.

Salinity Gradients. As can be seen in **Figures 3 A & B** increasing salinity using artificial seawater had a nonlinear effect on the amount of munitions sorbed by the sampler A significant increase in equilibrium partition constants occurred between 0 and 5 PSU though above 5 PSU changes in partition constants were small or negligible. EVA25 was impacted least by the change in salinity (a difference of 0.131 Log $K_{EVA\text{-}RDX}$ from 30 to 5 PSU), and had the lowest amount of sorbed TNT and RDX. The EVA80 sampler was impacted most by the initial change in salinity which supports a stronger sensitivity to changes in solubility of this sampler film. However the samplers were insensitive to salinity beyond this range.

Table 3: Uptake of Munitions by EVA25, EVA40 and EVA80. Temp Experiments in Milli-Q and Salinity (in artificial seawater)

EVA Type	Temperature ˚C	TNT (ug/g_{EVA})	RDX (ug/g_{EVA})	LOG KEVA TNT	LOG KEVA RDX	Salinity PSU	TNT (ug/g_{EVA})	RDX (ug/g_{EVA})	LOG KEVA TNT	LOG KEVA RDX
EVA25	25	0.136	0.029	1.143	0.372	30	0.263	0.046	2.010	1.554
EVA25	14	0.240	0.050	1.412	0.892	15	0.399	0.098	2.144	1.666
EVA25	4	0.299	0.063	1.796	1.537	5	0.335	0.066	1.935	1.423
EVA40	25	0.263	0.093	1.306	0.495	30	1.004	0.082	2.086	0.554
EVA40	14	0.326	0.149	1.512	1.092	15	1.177	0.129	2.286	1.507
EVA40	4	0.673	0.159	1.913	1.683	5	1.407	0.176	2.297	1.602
EVA80	25	0.550	0.301	1.430	0.663	30	1.824	0.287	2.444	1.860
EVA80	14	0.588	0.441	1.767	1.068	15	1.833	0.325	2.478	1.953
EVA80	4	0.890	0.561	1.951	1.753	5	2.358	0.483	2.409	1.941

***Figure 3A**: Log KEVA_TNT vs Salinity. EVA40_MQ and EVA40_34PSU come from the initial loading experiments and serve as a comparison.*

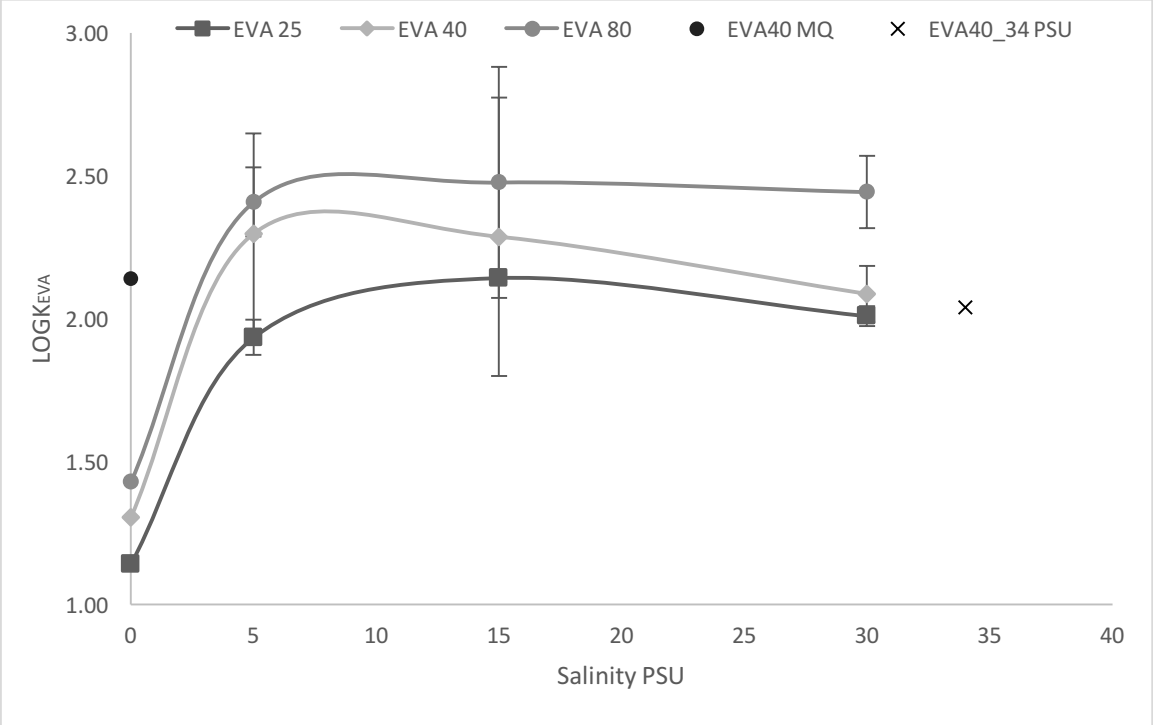

***Figure 3B**: Log KEVA_RDX vs Salinty. EVA40_MQ and EVA40_34PSU come from the initial loading experiments and serve as a comparison. EVA40_Outlier was an analytical outlier.*

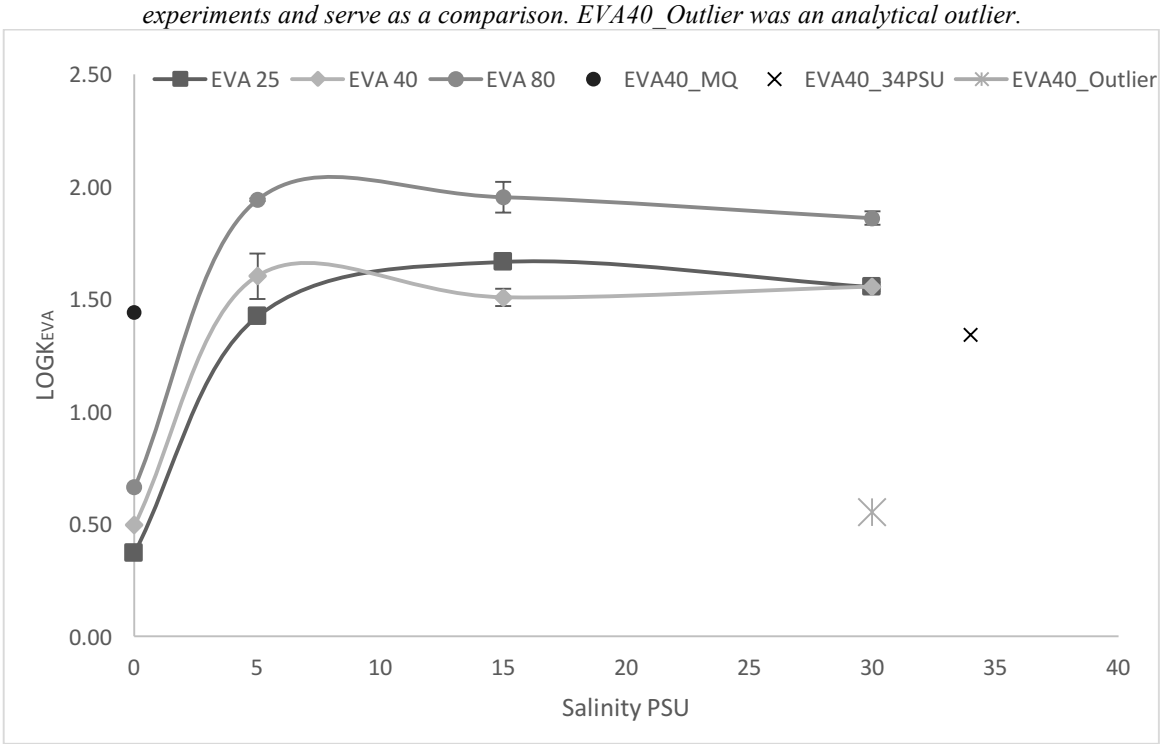

Comparison of Uptake Variation at Different temperatures. As can be seen from **Table 3**, uptake rates in milli-q varied with temperature and with the nature of the EVA polymer used. The EVA80 sampler was the most efficient (highest uptake) over all temperature ranges based on $\mu g/g_{EVA}$ concentrations normalized to the weight of EVA on the plates. Relative to the EVA80 uptake at equilibrium, at 25˚C, EVA25 only took up 25% of the TNT and 9% of the RDX, while EVA40 sorbed 48% of the TNT and 31% of the RDX. Again, relative to EVA80 in the 14˚C experiment, EVA25 sorbed 41% of the TNT and 11% of the RDX and EVA40 sorbed 55% and 34% of TNT and RDX, respectively. For the 4˚C experiment TNT uptake was 34% and 11% RDX for EVA25, and 76% TNT and 28% RDX uptake for EVA40 relative to EVA80's sorbed concentrations.

The log $K_{EVA/W}$ values derived from this experiment varied linearly with temperature as, seen in **Figure 4A** (TNT) and **4B** (RDX). EVA25 uptake was the most sensitive to temperature changes while EVA80 was the least. These trends imply that temperature corrections are polymer specific and in-field applications can be reasonably calibrated using equations **in Table 5**. The film integrity of the samplers was retained across the different temperatures. Log K_{EVA-W} is inversely proportional to temperature for both TNT and RDX across all acetate groupings. The amount sorbed by the samplers in ug/g_{EVA} followed this trend as a decrease in temperature resulted in an increase in amount of munitions sorbed for all EVA types. Thus as temperature decreases, the relative amount of munitions absorbed by the polymer increased linearly and can be reasonably accounted for.

Figure 4A: *TNT Uptake Kinetics: Log KEVA at 5, 15, and 25 ˚C*

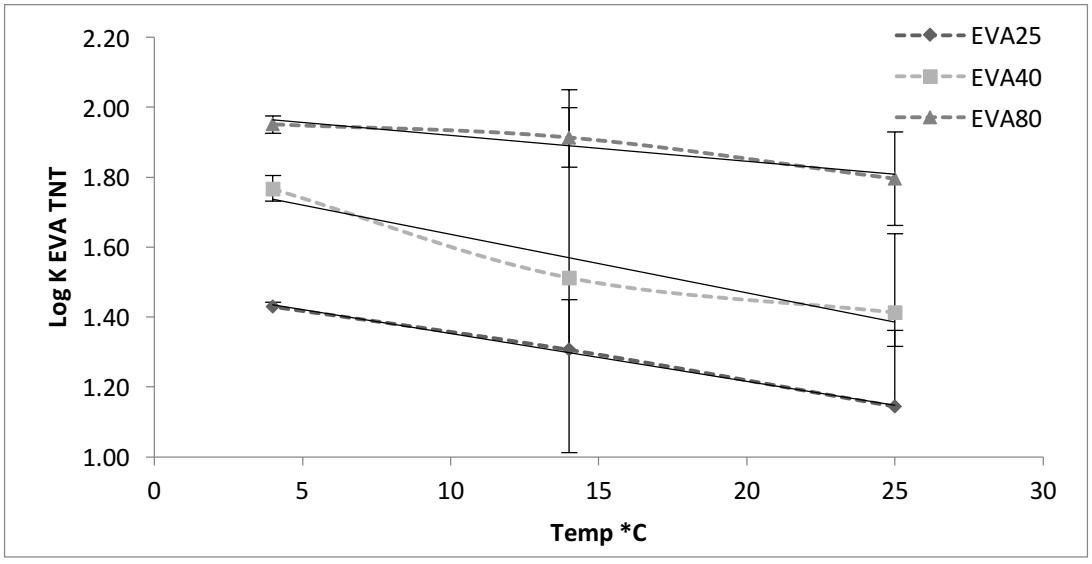

***Figure 4B**: RDX Uptake Kinetics: Log KEVA at 5, 15, and 25 ˚C*

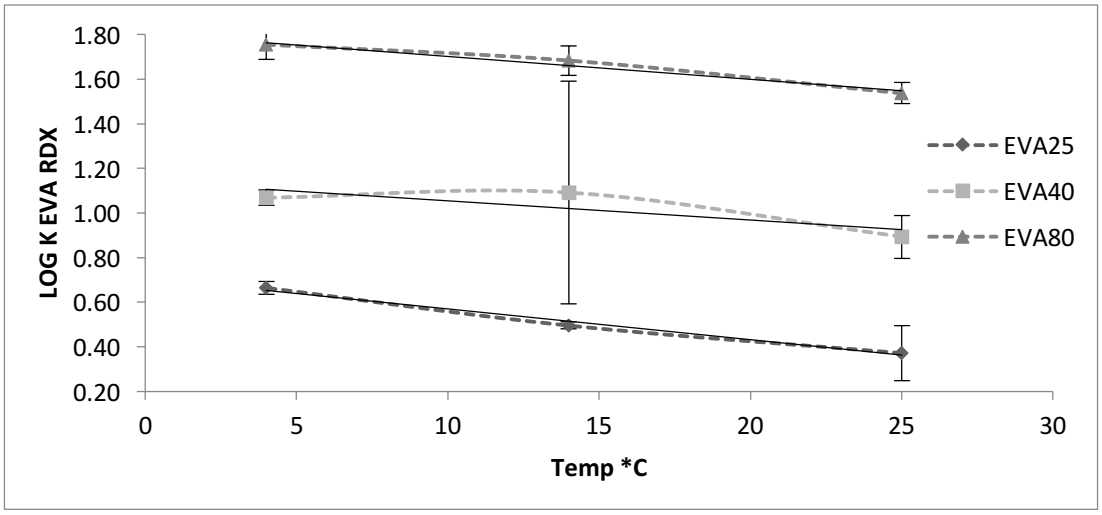

Table 4 shows the resulting equations for these relationships, as Log K_{EVA-W} by temperature. A strong correlation between a depression in LogKEVA-W as temperature increased was observed: as temperature increases, less munitions sorb to the sampler. All R^2 values were above 0.926, except for the EVA40 RDX correlation, which was slightly weaker at an R^2 of 0.677, showing a greater temperature dependence. This depression was similar across the different EVA types, showing a definite temperature dependence, but that the changes in temperature affect each of the EVA types slightly differently.

***Table 4**: Slopes and R^2 Values for TNT and RDX across EVA types for temperature experiment (T=5-25˚C) in Milli-Q (Companion figures: 3A & 3B).*

	TNT		RDX	
	Equation	R^2	Equation	R^2
EVA80	y=-0.007x+1.993	0.9328	y=-0.010x+1.806	0.9710
EVA40	y=-0.002x+1.804	0.9261	y=-0.009x+1.140	0.6774
EVA25	y=-0.014x+1.489	0.9973	y=-0.014x+0.708	0.9863

Linear Free Energy Relationships. Based on the linear free energy relationships (LFER) of EVA there is a predicted increase in the affinity for TNT and RDX of 0.010 and 0.006 logarithmic units per percent acetate unit increase for TNT and RDX respectively. This is consistent with a chemical thermodynamic basis for the improved affinity for TNT and RDX with increased frequency of vinyl acetate substitutions. A likely explanation for this more

efficient sorption is the higher polarity that results from an increase in acetate composition of the polymer, and a lower fugacity of the TNT and RDX in EVA than in other reference hydrophobic media such as octanol or polyethylene.

Equilibrium partitioning constants increased consistently with the % acetate in the polymer. This applied to both TNT and RDX across all temperatures (**Tables 3 and 5**). The impact of the increased % acetate to partitioning of these relatively soluble organic compounds was examined in these tables (**3 & 5**); there is a remarkable consistency in the influence of the acetate group. This implies that the polar acetate groups are likely facilitating sorption of TNT and RDX in the polymer and a likely sorption mechanism may include dipole-dipole interactions between the nitrate groups and vinyl acetate.

Table 5: Comparison of Partitioning Coefficients.

		Temperature KEVA Average			Salinity KEVA Average		
Compound	Log Kow	KEVA25	KEVA40	KEVA80	KEVA25	KEVA40	KEVA80
TNT (2,4,6-trinitrotolulene)	1.98	1.29	1.56	1.89	2.03	2.22	2.44
RDX (hexahydro-1,3,5-trinitro-1,3,5-triazine)	0.87	0.51	1.02	1.66	1.55	1.22	1.92

Utilizing the equilibrium constants derived from the K_{EVA} values reported in **Table 3**, the Gibbs free energy was calculated using **equations 1** and **2,** and **Figures 5A & 5B**. A linear regression was performed on the data for both TNT and RDX, resulting in the Y-axis intercept interpreted as ($\Delta S^{\circ}/R$), and the slope interpreted as ($-\Delta H^{\circ}/R$), assuming that these values are temperature independent. By multiplying by the thermodynamic constant (R) of 8.314 J mol^{-1} K^{-1}, values for enthalpy (ΔH°) and entropy (ΔS°) were calculated for each EVA type in equations (1) and (2). The results are summarized **in Table 6**. Note this analysis helps identify that the increase in vinyl acetate substitution results in an entropic gain of 2.8% and enthalpic gain of 5.2% for every additional 10% compositional increase of vinyl acetate added in the film.

1.) $\Delta G^{\circ} = \Delta H^{\circ} - T\Delta S^{\circ}$

2.) $\Delta G = -RTlnK_{EVA}$

Figure 5A: *TNT Enthalpy and Entropy Derivations*

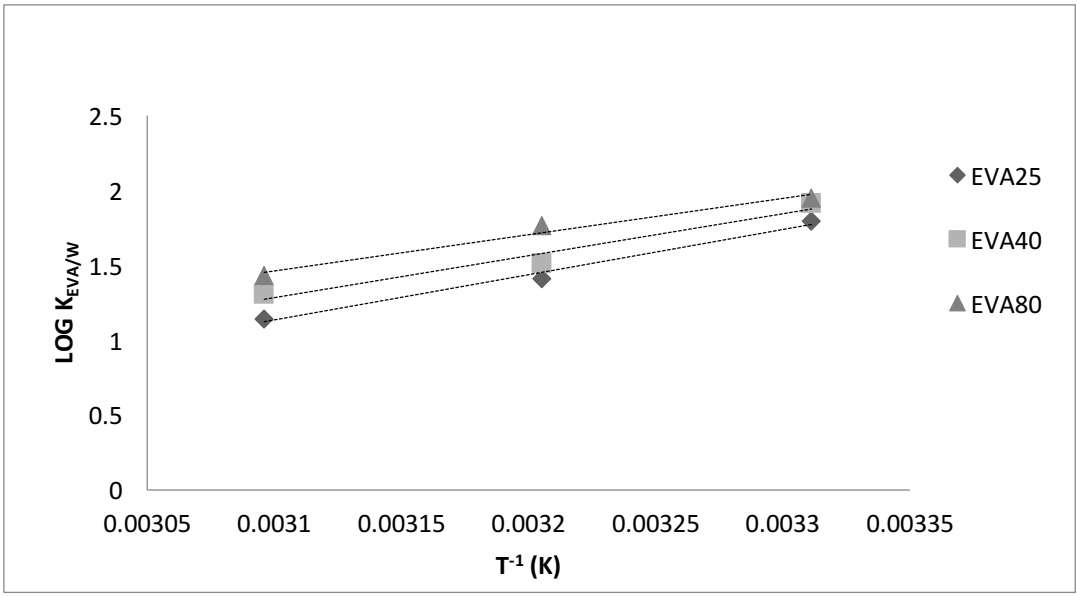

Figure 5B: *RDX Entropy and Enthalpy Derivations*

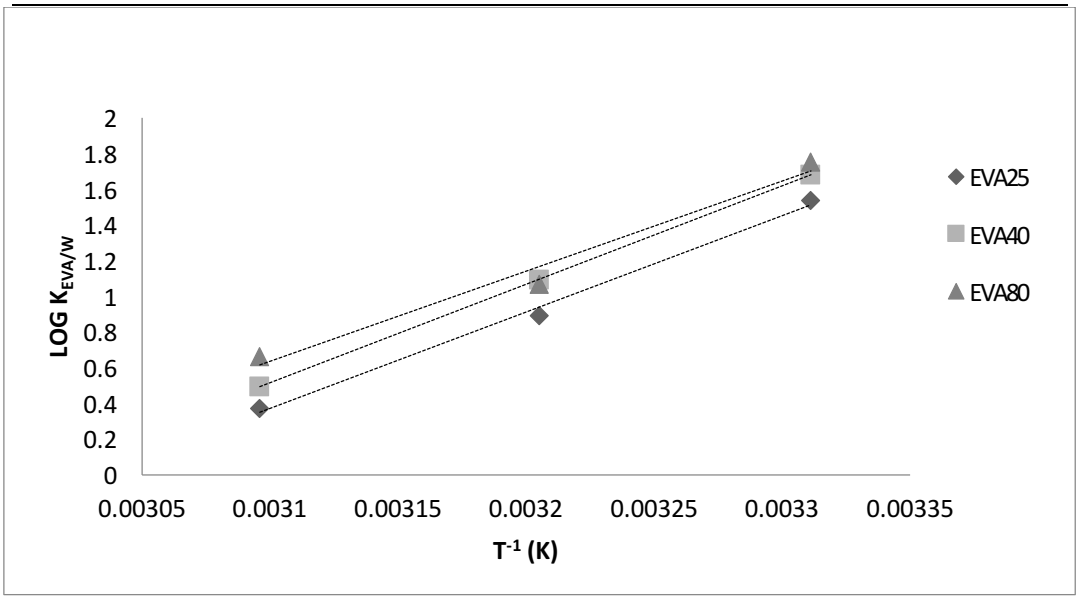

Table 6: Comparison of thermodynamic coefficients.

	TNT					RDX				
	Y Int (dS/R)	Slope (-DH /R)	r^2	dH	dS	Y Int (dS/R)	Slope (-DH /R)	r^2	dH	dS
EVA25	-6.05	3031	0.9747	-25201.1	-50.302	-15.0	5408	0.9761	-44962.1	-124.71
EVA40	-7.44	2815	0.9638	-23405.2	-61.860	-16.6	5518	1.0000	-45876.6	-138.01
EVA80	-8.26	2423	0.9881	-20145.9	-68.677	-16.4	5057	0.9951	-42043.8	-136.34

EVA Composition Comparison. The lowest percent acetate polymer in this study, EVA25, was able to sorb both TNT and RDX, although in much lower amounts than the EVA40 and EVA80. As the ratio of vinyl acetate to ethylene in the polymer increases, the relative amount of munitions sorbed also increases (**Table 3**). RDX appears to respond more to the change in EVA film polarity than TNT.

The EVA80 admixture, due to its dispersive properties and additives, is more difficult to dissolve into DCM but is equivalent to the other EVA types in regards to blanks and control samples. It was shown that this mixture was the most effective at sorbing TNT and RDX, but its resistance to solvation and lower elasticity make it a less favorable film. While it retains some thermoplastic properties of the lower percent acetate mixtures, it does not seem to readily contract or expand as the EVA40 mixture does. Nonetheless its increased affinity for RDX may be useful in some applications.

EVA40, the more thoroughly studied of the polymers in this experiment, was able to sorb TNT and RDX more readily than the EVA25 sampler. Much like the EVA25 sampler, RDX partitioned to a relatively lesser extent than TNT, despite its lower solubility in water, likely due to differences in polarity between the molecules. The KEVA/W's of RDX are however greater than the K_{OW}'s and thus RDX has a higher affinity for EVA than octanol. Use of the EVA40 sampler is an all-around best choice for its coating ease, film thickness, film integrity, how readily it dissolves in relatively un-harmful solvents (DCM, Hexane/Ethyl-acetate mixtures, etc), thermoplastic properties, and chemical affinities. EVA40 should be considered a useful middle ground, and should be used for exploratory work in which a wide range of compounds might be present . In terms of averaged $\log K_{EVA}$ values from the temperature experiments **(Table 4)**, the EVA80 mixtures RDX partitioning was much higher than the accepted Log K_{ow} value of 0.87 (1.66), as it was for EVA40 (1.02) in the temperature experiment as well. For TNT, both the $\text{Log}K_{EVA40}$ (1.563) and Log K_{EVA80}(1.887) were close to the accepted $\text{Log}K_{ow}$ value of 1.98.

Future Work

As the caches of dumped munitions from wartime campaigns are losing their structural integrity from environmental processes, leaching is occurring at a rate that is yet to be fully

understood. In addition, the rate at which high energy munitions are released into the environment via wastewater from production or deposition into the environment from test-ranges needs to be constantly assessed at a multitude of sites. Therefore, the need for a rapid, accurate assessment of the compounds present must become priority. While detecting sensors are being developed, they do not yet have the ability to quantify in the same manner that the EVA passive sampler is able to. Most of the available passive sampling technology on the market is selective towards the polar, or non-polar fraction of pollutants, while EVA can sorb across a wide range of polarities.

Aside from being a viable platform for global sampling regimes, the low cost, low toxicity, and robust film coating of ethylene vinyl-acetate based samplers makes them ideal for localized sediment, water, or atmospheric sampling. As the geometry of the sampling device can be changed to almost anything able to maintain its integrity in methylene chloride, specialized samplers for local problems can be developed.

Acknowledgements

This work was funded by the Joint Department of Defense, Department of Energy and the Environmental Protection Agency's SERDP-SEED Program Award ER2539. We would like to thank Jessica Hinckley (Uconn) for help processing samples, and David Cady for analytical support.

REFERENCES

1. Ariyarathna, Thivanka, Vlahos, Penny, Tobias, Craig, Smith, Richard. "Sorption Kinetics of TNT and RDX in Anaerobic Freshwater and Marine Sediments: Batch Studies." *Environmental Toxicology and Chemistry.* 2015

2. Ballentine, Mark., Tobias, Craig., Vlahos, Penny., Smith, Richard W., Cooper, Christopher. "Bioconcentration of TNT and RDX in Coastal Marine Biota." *Archives of Environmental Contamination and Toxicology* 2014. Vol 67.

3. Drzyzga, O., Gorontzy, T., Schmidt, A., Blotevogel, K.H. "Toxicity of Explosives and Related Compounds to the Luminescent Bacterium *Vibrio fischeri* NRRL-B-11177." *Archives of Environmental Contamination and Toxicology* 1995. Vol 28: 229-235.

4. Kalderis, Dimitrios., Juhasz, Albert L., Boopathy, Raj., Comfort, Steve. "Soils contaminated with explosives: Environmental fate and evaluation of state-of-the-art remediation processes (IUPAC Technical Report)." *Pure Appl. Chem.* 2011. Vol 83: 1407-1484

5. Phillips, Carlton T., Checkai, Ronald T., Kuperman, Roman G., Simini, Michael, Kolakowski, Jan E., Kurnas, Carl W. "Environmental Toxicity of the Explosives RDX and TNT in Soil to the Soil Invertebrate *Folsomia Candida*." Internal Report, US Army Edgewood Chemical Biological Center, 2004

6. Raub, Kristen B., Vlahos, Penny, Whitney, Michael. "Comparison of marine sampling methods for organic contaminants: Passive samplers, water extractions, and live oyster deployment." Marine Environmental Research, 2015. Vol 109: 148-158

7. Smith, Richard W., Vlahos, Penny., Tobias, Craig., Ballentine, Mark., Ariyarathna, Thivanka., Cooper, Christopher. "Removal Rates of Dissolved Munitions Compounds in Seawater." *Chemosphere* 2013. Vol 92: 898-904.

8. Smith, Richard W., Tobias, Craig., Vlahos, Penny., Cooper, Christopher., Ballentine, Mark., Ariyarathna, Thivanka., Fallis, Stephen., Groshens, Thomas J. "Mineralization of RDX-Derived Nitrogen to N2 via Denitrification in Coastal Marine Sediments." *Environmental Science & Technology* 2015. Vol 49: 2180-2187.

9. St. George, Tiffany., Vlahos, Penny., Harner, Tom., Helm, Paul., Wilford, Byrony. "A rapidly equilibrating, thin film, passive water sampler for organic contaminants; Characterization and field testing." *Environmental Pollution* 2011. Vol 159: 481-486

10. Tucca, Felipe., Moya, Heriberto., Barra, Ricardo. "Ethylene vinyl acetate polymer as a tool for passive sampling monitoring of hydrophobic chemicals in the salmon farm industry." *Marine Pollution Bulletin* 2014: Vol 88: 174-179.

11. Yinon, J. "Toxicity and Metabolism of Explosives." CRC Press: Boca Raton, FL, 1990

CHAPTER 3. A novel *in-situ* sulfate sampler for aquatic systems

Penny Vlahos[a]*, Joseph Warren [a], Jennifer Houghton[b], David A. Fike[b]

[a]Department of Marine Sciences, University of Connecticut, 1080 Shennecossett Rd. Groton CT 06340 USA; [b]Department of Earth and Planetary Sciences, Washington University, CB 1169, 1 Brookings Dr., Saint Louis, MO 63130-4899 USA

***Corresponding author: penny.vlahos@uconn.edu; +1 (860) 235-5337**

Published: ACS Earth and Space Chemsitry (DOI: 10.1021/acsearthspacechem.7b00012) on 11 April, 2017.

Abstract

High-resolution records of porewater sulfate concentrations are critical to understanding the modern biogeochemical sulfur cycle, particularly the connection between microbial metabolic activity, ambient geochemistry and feedbacks on global carbon cycling and climate. To date, the nature of sulfate measurements requires extraction of fluids or sediments from the field, often leading to significant disturbances in the systems studied. Further, the resulting data may have limited spatial resolution (due to volume restrictions of porewater sampling), hindering the ability to reconstruct key biological and geochemical processes. Here a novel passive sampler that is seeded with barium oxalate is optimized for the *in-situ* sampling of sulfate to improve both the fidelity and the spatial resolution of sulfate profiles that may be obtained. Simulated sediment studies showed that consistent profiles could be resolved in both 2 and 6 hour deployments that were in good agreement with traditional porewater reconstructions from adjacent core samples. Although the sampler has been calibrated for water concentrations between 2 to 28 mM of sulfate, the detection limits may be improved with modified sampler geometry or longer deployment times.

Highlights [3-5, max 85 characters each]

- The design and testing of an *in situ* porewater sulfate sampler is described
- Sampler profiles agree well with traditional profile methods
- Captured sulfate can be extracted for subsequent isotopic analysis
- Captured sulfate is amenable to *in situ* isotopic analysis by SIMS

Keywords

sulfate isotopes, sulfate sampling, sulfate sampler, passive sampling, marine sulfate

Abbreviations

BaOrg – organically complexed barium: barium oxalate, barium citrate and barium stearate

BaO – barium oxide

BaOx – barium oxalate

EDS - energy-dispersive X-ray spectroscopy

EVA – ethylene vinyl acetate

NEG - normal-incidence electron flood gun

SEM – scanning electron microscopy

SIMS - secondary ion mass spectrometry

TCD - thermal conductivity detector
‰ - permil
V-CDT - Vienna Canyon Diablo Troilite

INTRODUCTION

The biogeochemical sulfur cycle is intricately linked to a number of elemental cycles and the resulting fate and transport of these elements depends on understanding reaction consortia that are currently not well constrained. Sulfur is abundant in the marine environment as sulfate (28 mM), playing a major role in regulating marine redox chemistry and the metabolic activity of multiple microbial pathways (e.g., sulfate reduction, disproportionation, and sulfide oxidation)[1]. The sulfur cycle is directly connected to the carbon biogeochemical cycle and to climate via many routes that include the remineralization of organic carbon to CO_2. Microbially mediated sulfate-reduction in marine sediments can account for up to 90% of carbon mineralization[2], and therefore strongly regulates carbon burial in these environments.

Characterization of sulfur cycling in modern environments is ideally accomplished by parallel analysis of geochemistry (e.g., sulfate and sulfide abundance and isotopic composition), microbial ecology and metabolic activity. Individual geochemical measurements (e.g., sulfide profiles without corresponding sulfate records) can often be interpreted in multiple ways, making definitive reconstructions of (paleo) environmental conditions and microbial ecology challenging. In particular, the link between μm-scale microbial activity that drives biogeochemical cycling and the resulting geochemical consequences of this activity have remained elusive, in large part because of the difficulty of extracting sufficient material for geochemical analyses at small scales. Coupled, spatially resolved measurements of sulfate and sulfide are needed to better constrain microbial sulfur cycling in aqueous and sedimentary systems and to better understand the underlying links to carbon cycling and climate[1]. Recent advances have enabled the capture and subsequent analysis of hydrogen sulfide at μm-scales. This 2D mapping of sulfide profiles allows

for new insights into microbial sulfur cycling[3,4,5]. However, similar approaches to capturing ambient sulfate, while preserving its spatial information, have been lacking.

Here we describe the development of a novel sulfate sampler that may be used alongside sulfide films[6] to collect and immobilize sulfate ions, enabling the spatial mapping of sulfate *in situ* with minimal disturbance to the sediments and at higher resolution than is possible with standard coring and porewater extraction methods. The sampler design is based on a passive sampling device[7,8] which uses an ethylene-vinyl acetate (EVA) thin film coating on a substrate for the collection of organic compounds in aquatic systems. When placed in solution, including porewaters within sediments, dissolved compounds readily diffuse into the EVA film and can later be extracted for analysis. Barium ions precipitate as barium sulfate (barite: $BaSO_4$) in solutions containing sulfate; the resulting barite remains insoluble in water and organic solvents, making barium an ideal cation for trapping sulfate as a solid that can be either subsequently extracted from the film or analyzed *in situ* within the film using scanning electron microscopy (SEM) or secondary ion mass spectrometry (SIMS). The modified thin film design (St. George et al. 2008) was seeded with a barium-containing organic compound (BaOrg), using an organic ligand with a high affinity for the EVA coating. The ideal BaOrg compound must readily capture sulfate by anion exchange, yet not compromise the integrity of the EVA thin film. Achieving parallel sulfide and sulfate *in situ* sampling will enable the simultaneous collection of these sulfur species in sediment porewaters and improve the current understanding of sulfur cycling in many modern systems.

METHODS

Materials

Ethylene Vinyl-Acetate pellets were sourced from Sigma Aldrch (EVA 40%, 25% Acetate by weight) and Polysci (EVA 80%). The organic barium-containing compounds were sourced as follows: stearate (Pfaltz & Bauer), citrate (MP Chemical), oxalate (Accela). Sodium sulfate, methylene chloride (DCM), acetone, methanol UHP, and hydrochloric acid (ACS, 12N) were purchased from Fisher Optima.

Preparation of EVA thin-film sulfate sampler

Solutions of each EVA-BaOrg combination were prepared in dichloromethane (DCM). EVA and BaOrg were added to 400 ml DCM to achieve 60 mM concentrations for each. The suspension was coated by dipping and later replaced by spraying (for a more uniform coating) onto the substrate and allowed to air dry in a fume hood to completely evaporate the DCM then reweighed to determine the mass and thereby the moles of barium in the coating. Spraying produced a more uniform coating that could be adjusted based on the target barium amount. The choice of substrate to coat could be tailored to the needs of the application; however, copper sheets were used in this study due to its antifouling properties, and the malleability of the material including the ease with which it could be cut into subsections. The flat geometry was chosen in order to minimize damage to the sediments and for ease of introduction into the sediments (blade-like)

Calibration experiments

Feasibility experiments to determine the best organic ligand for sulfate were conducted in triplicate in aqueous solutions made in DI water. Plates were coated in EVA and seeded with 60 mM each of barium oxalate, barium citrate, and barium stearate. This concentration was chosen to achieve a 1:1 BaOrg:EVA mole ratio. Plates were then exposed in 1 L of sodium sulfate solutions of 5,

10, and 28 mM. After 48 hours, the plates were removed and extracted to isolate any $BaSO_4$ that formed in the film. The combined parameters of strength of coating (e.g., resistance to tearing during deployment), purity of $BaSO_4$ product extracted, and ability to capture sulfate (both $BaSO_4$ yield and efficiency) were used to evaluate each BaOrg compound. The % purity of the extracted $BaSO_4$ product was measured by a thermal conductivity detector (TCD) after combustion to SO_2 gas. The yield of $BaSO_4$ was calculated on a mass basis ($g_{coating}$) as follows:

$$Yield = \left(\frac{mmoles_{BaSO4}}{g_{coating}}\right) = \left(\frac{(g_{BaSO4})(\%purity)}{g_{coating}}\right)\left(\frac{1000}{m.w._{BaSO4}}\right) \quad (1)$$

The efficiency of each barium compound to capture sulfate was calculated as a percentage of available Ba converted to $BaSO_4$ as follows:

$$Efficiency(\%) = \left(\frac{mmoles_{BaSO4}}{mmoles_{BaOrg}}\right)(100) \quad (2)$$

Based on these parameters in initial coating experiments, barium oxalate (BaOx) was determined to be most suitable for a sampling device and was used exclusively in all subsequent testing (see below).

The polarity of EVA film was examined. EVA may be adjusted by the ethylene to acetate ratio in the polymer. In order to examine differences that this ratio could cause, three different commercial types of EVA containing 20, 40 and 80 % acetate by mass were tested by coating plates with BaOx in each EVA type, incubating the plates for 48 h with 28 mM SO_4^{2-} solutions and comparing yields.

The optimum concentration of BaOx was then determined by testing replicates of EVA thin films seeded with 100, 200, and 300 mM BaOx. Time-series measurements of sulfate uptake onto the films were tested in triplicate in separate 28 mM Na_2SO_4 solutions for 2 to 72 hours. The rate of

sulfate uptake into the film as a function of the concentration of sulfate was determined in both fresh and saline (artificial seawater at 30 PSU) solutions. For time series, sampler uptake of sulfate was confirmed by assessing residual sulfate abundance in 40 ml water samples taken from the solution periodically. The sulfate concentration was determined using a gravimetric method of precipitating barium sulfate using 5 ml of 0.1 g/ml barium chloride solution ($BaCl_2$). The solution contained an excess $BaCl_2$, thus ensuring quantitative removal of sulfate as $BaSO_4$. This was retained by a GFF filter, washed several times to remove any excess $BaCl_2$, and then dried overnight at 90^{o}C before a final weight was determined[9]. An additional sampler set with a 200 mM BaOx layer protected by an outer layer of pure EVA (no BaOx) was also tested to examine possible benefits of a retaining layer. Based on these experiments, 200 mM was determined to be the optimal concentration of BaOx for the sampling device and was used exclusively in all subsequent testing (see below).

Uptake of Sulfate

The rate of uptake was measured for the optimized sampler film (200mM barium oxalate, 40% acetate EVA) in solutions of variable sulfate concentrations (1, 5, 10, 20, 28mM sulfate) using the same gravimetric method described. Uptake rate vs sulfur isotopic fractionation was also evaluated over the uptake experiment by determining the sulfur isotopic composition in the film and the protocol outlined in Figure S1.

Sulfate extraction for bulk analysis

The thin-film coating was dissolved off the substrate in a sealed jar in excess (200 ml) DCM for 8 to 12 hours. The extract volume was reduced with a gentle stream of nitrogen to approximately 3

ml and transferred to a glass test tube. The solid barium residue was recovered by centrifugation and then triple rinsed in DCM (3 ml) with 5 minutes of sonication between each rinse to remove any soluble EVA. At this stage, the solid residue contained a mixture of $BaSO_4$, other barium compounds captured *in situ* (the most common being $BaCO_3$ or $BaPO_4$), and residual BaOrg. To improve extract purity, the solid residue was treated with 12N HCl (4 ml) and 3% hydrogen peroxide (3 ml) and sonicated for 2 hours to remove acid-volatile Ba compounds and oxidize the original organic ligand (in this case oxalate, $C_2O_4^{2-}$):

$$C_2O_4^{2-}\,(aq) + H_2O_2\,(aq) + 2H^+\,(aq) \rightarrow 2CO_2\,(g) + H_2O\,(aq) \qquad (3)$$

Effervescence was caused by the conversion of the organic ligand (e.g., oxalate in eq. 3) to CO_2, as well as reactions from other impurities such as carbonate. The sample was centrifuged for 15 min and the liquid decanted. This purification step was repeated at least two additional times or until effervescence ceased. After the final decantation, the remaining $BaSO_4$ precipitate was rinsed and sonicated with deionized water to remove any barium chloride that may have precipitated from excess barium in the HCl solution, and centrifuged for ten minutes. The sample was then rinsed with acetone twice to remove water, spinning down each rinse for at least ten minutes. After the final rinse, the dried precipitate was combusted for purity and bulk $\partial^{34}S$ analysis as described below. The optimized extraction procedure is summarized in Figure S1.

Bulk sulfur isotopic analysis

The barium sulfate precipitate extracted from thin films was analyzed for compound purity and isotopic composition by combustion to SO_2 on a Costech ECS 4010 Elemental Analyzer (Costech Analytical Technologies Inc., Valencia, California, USA) and measured on a Thermo Delta V Plus Isotope Ratio Mass Spectrometer (Thermo Finnigan, Bremen, Germany) at Washington

University. Purity of the extract was determined by comparing the area of the evolved SO_2 peak measured by TCD to a barium sulfate standard curve, with a resulting precision of ± 1% (1σ). The evolved SO_2 was then passed through a Thermo Scientific Conflo IV interface to a Thermo Scientific Delta V Plus mass spectrometer for isotopic analysis. Sulfur isotope values are reported in permil (‰), relative to the V-CDT (Vienna Canyon Diablo Troilite) scale. Based on replicate analyses across several days, reproducibility of sulfur isotope measurements is ~0.3‰ (1σ).

High-resolution thin-film characterization

SEM imaging of the surface of carbon-coated, barium oxalate-seeded, EVA thin films, was performed at the Nano Research Facility, Washington University in St. Louis. Images were collected using an FEI Nova NanoSEM 230 (15kV accelerating voltage, working distance of 4.5 mm, spot size of 4.5 nm) to determine the surface topography. The distribution of BaOx and $BaSO_4$ on the micron scale was measured by energy-dispersive spectroscopy (EDS) to verify the elemental composition of surface features, comparing films prior to and post exposure to sulfate solutions.

SIMS analysis was performed on a Cameca IMS 7F-GEO at Washington University in St. Louis to analyze the elemental composition with depth into the thin film. Eight to ten depth profiles were measured on random locations across each thin film using a Cs^+ primary ion beam, accelerated at 10 kV with an intensity of 12 nA (Gaussian mode with a primary beam aperture of 400 μm). The beam was scanned over a 100 × 100 μm area during analysis, applying a physical gate of 62.5 μm to reduce edge effects created by the sidewalls of the craters. Samples were coated with 50 nm of gold prior to analysis and the normal-incidence electron flood gun (NEG) was used to neutralize

positive charge buildup in the analysis area. Negative secondary ions were extracted with a -10-kV potential. The field aperture was set to 750 μm, entrance slit was at 11.9 μm, and the mass resolving power was 3000. Abundance of ^{12}C, ^{16}O, ^{32}S, ^{63}Cu and $^{138}Ba^{16}O$ were measured in mono-collection mode using magnet switching to allow analysis of the desired masses using two Faraday cups and an electron multiplier (for BaO). Profiles were measured down to the depth at which the underlying copper became abundant, indicating complete sputtering through the EVA thin film. The abundance of sulfur was normalized to the sum of matrix-level components (e.g., carbon and oxygen from the EVA polymer) to allow direct comparison between pieces of film exposed to different concentrations of sulfate for different amounts of time. Depth within the film is reported as a fraction of total cycles to normalize for differences in the thickness of the thin film, which varied at each location profiled. Normalized depth profiles were combined for each film and the average and standard error of concentration was determined at each depth.

Verification of sulfate capture relative to BaOx abundance was determined using a combined SIMS and SEM-EDS imaging approach. Images with SIMS were acquired after pre-focusing the beam on the sample in a test area, adjusting the z-axis of the stage as necessary. All elements are imaged with the electron multiplier with a wait time (s) to count time (s) ratio of 2:1 for ^{12}C and ^{16}O, 2:5 for ^{32}S and ^{63}Cu, and 2.5:30 for $^{138}Ba^{16}O$. Magnet calibration was completed after a long period (>5 minutes) of cycling prior to accepting peak positions. The $^{138}Ba^{16}O$ peak height during this process is monitored to be sure the signal does not saturate the electron multiplier (i.e., ~10^6 counts/s), with the entrance slit adjusted as required. After this set up procedure, the stage is moved 200 μm to a fresh area of film close enough to maintain the same beam conditions. A final beam center is performed on this new spot while the magnet cycles before the DTOS is turned off for the analysis. Image acquisition is performed following a 100 s pre-sputtering period at 100 x 100

μm and 8 nA, with images collected over a 100x100 μm raster with a physical gate of 62.5 μm diameter at 8 pA. A repeated sequence of image acquisition followed by rapid sputtering was used to create a depth profile of high resolution images into the thin film. Once a crater had been created in SIMS, the film was imaged with SEM-EDS to map the sulfur, barium and carbon concentration at the base of the crater for direct comparison between the two techniques. SIMS analysis of Ba abundance was based on the abundance of a BaO ion (detectable with the Cs+ primary beam). Because the abundance of this diatomic ion can reflect changes in matrix (e.g., O abundance) as well as Ba abundance, the profiles should only be interpreted qualitatively. EDS is able to directly measure Ba and these results from the base of the SIMS craters were used to correct the SIMS $^{138}Ba^{16}O$ counts. The SEM image was aligned to the SIMS image and cropped so that each image was 256x256 pixels of superimposed locations centered on a large $BaSO_4$ clump. Smaller areas (30x30 pixels) on each image were selected randomly within the clump and the average counts of S and Ba (for SEM) and S and $^{138}Ba^{16}O$ (for SIMS) were calculated in ImageJ (NIH). The ratio of SEM counts: SIMS counts was determined for each small area as a correction factor. For S, the average correction ratio was 0.91 (s.d. 0.05, n=4) and for $^{138}Ba^{16}O$, the average correction ratio was 2.23 (s.d. 0.34, n=4). The counts in the SIMS images were then multiplied by these correction factors in ImageJ to obtain a corrected SIMS image.

Sediment Columns

Experiments to test the ability of thin-film samplers to reproduce a known vertical profile of sulfate concentrations and isotopic composition were conducted in laboratory sediment columns. Thin-film samplers were prepared by coating 10 cm wide copper ribbon with the EVA/BaOx coating. A sediment column was assembled in a cylinder pierced at regular intervals with Rhizon pore water samplers (Rhizosphere Research Products B.V., Wageningen, Netherlands). Thin-film

samplers were imbedded in a column of layers of quartz sand (<1.17 mm grain size) that were successively saturated with known mixtures of two end-member solutions, each containing a different anion tracer (30 mM SO_4^{-2}, $\partial^{34}S$: -4‰, 13 mM Br^- and 5 mM SO_4^{-2}, $\partial^{34}S$: +40‰, 13 mM Cl^-) to create a chemical gradient. An aliquot of each mixture was preserved with excess $BaCl_2$ for isotopic analysis. Filtered porewater samples (0.1 ml after discarding a 0.1 ml volume to prime the Rhizon) were collected through the Rhizons over time to monitor the change in chemical gradient by quantifying Br^-, Cl^- and SO_4^{-2} by ion chromatography (Metrohm 881 Compact IC, with suppression using an A Supp 5-100 column with conductivity detection). After 7.5 hours, the experiment was ended and porewater samples (3.5 ml after a 0.1 ml discarded bleed) were collected for both anion analysis by ion chromatography and sulfur isotopic analysis of precipitated $BaSO_4$. The thin-film samplers were removed from the sediment column and cut into 2 cm strips (total surface area of 20 cm^2) for individual extraction of the captured $BaSO_4$. The extracted $BaSO_4$ was analyzed for isotopic composition and compound purity as described above.

RESULTS AND DISCUSSION

Selection of organic barium for film:

Three barium-containing organic compounds (barium oxalate, barium citrate and barium stearate) were investigated for their potential to capture sulfate diffusing into the thin film. The organic barium compounds were selected to evaluate both the effect of organic ligand size on film integrity and the number of Ba atoms per molecule on the precipitation efficiency. Each thin film was incubated in 5, 10, and 28mM sulfate solutions for 48 hours and the amount of $BaSO_4$ extracted from the films was compared to the maximum theoretical $BaSO_4$ yield. The pure EVA coatings showed no detectable $BaSO_4$ precipitate or free sulfate remaining after the extraction process in

any treatments (Table 1). The absence of significant diffusive capture of sulfate in the controls (pure EVA films) was confirmed by adding $BaCl_2$ to the initial DCM extract. The lack of $BaSO_4$ precipitate validated the role of the ethylene vinyl acetate as a non-competing diffusive film whose permeability to sulfate diffusion did not result in competing sulfate precipitates. In addition, the blank (0 mM SO_4) controls with all organic Ba compounds had no detectable precipitate. Sulfate was detectable even in 5 mM sulfate solutions in all three EVA/BaOrg films. Barium stearate films captured the least amount of sulfate (on a per mole Ba basis), had the lowest purity after extraction, and made the least stable and uniform coating (Table 1). Although the greatest yield on a mole to mole basis was with barium citrate, the $BaSO_4$ was difficult to purify and the stability of the film coating was poor (Table 1). In contrast, barium oxalate formed a very homogeneous film, likely due to the smaller size of the oxalate, and resulted in higher purity yields (Table 1). Barium oxalate was therefore chosen as the additive of choice and all subsequent optimizations focused on this film composition.

Table 1: Recoveries of four coatings exposed to 5, 10 and 28mM sulfate solutions for 48 hours. The standard deviation of replicates (n) is shown in brackets next to the averages for each test. All barium-free controls were below detection (b.d.) for extractable barium sulfate.

SO_4 (mM)	***% purity of $BaSO_4$ extracted***	***Yield (mmoles SO_4/g coating)***	***Efficiency (% Ba converted to $BaSO_4$)***	***Film quality***
Ethylene vinyl acetate (control) $((CH_2CH_2)_6[CH_2CH(OCOCH_3)]_2$, m.w. 342.43)				
5 (n=3)	b.d.	b.d.	b.d.	Good
10 (n=3)	b.d.	b.d.	b.d.	Good
28 (n=3)	b.d.	b.d.	b.d.	Good
Barium oxalate (BaC_2O_4, m.w. 225.34)				
5 (n=3)	35.0 (32.8)	0.053 (0.039)	3.0 (2.2)	Good
10 (n=3)	79.7 (3.1)	0.298 (0.054)	16.8 (3.1)	Good
28 (n=3)	14.1 (4.7)	0.141 (0.037)	8.0 (2.1)	Good
Barium citrate $((C_6H_5O_7)_2 \bullet Ba_3 \bullet 7H_2O$, m.w. 916.32)				
5 (n=3)	20.8 (3.5)	0.286 (0.021)	21.8 (1.6)	Poor
10 (n=3)	32.3 (5.2)	0.549 (0.171)	41.9 (13.1)	Poor
28 (n=3)	14.3 (0.8)	0.267 (0.115)	20.4 (8.8)	Poor
Barium stearate ($C_{36}H_70BaO_4$, m.w. 704.28)				
5 (n=3)	1.2 (1.1)	0.0031 (0.0036)	0.5 (0.6)	Poor
10 (n=3)	0.9 (1.0)	0.0165 (0.0145)	2.9 (2.5)	Poor
28 (n=2)	3.2 (0.4)	0.0079 (0.0045)	1.4 (0.8)	Poor

Polarity of EVA film:

In order to further improve sulfur uptake, the composition of the EVA polymer film was tested when it was composed of 40% by mass acetate and 80% by mass acetate (i.e., producing a more polar film). The results show a clear increase (> 2.5x) in uptake of sulfate by the EVA 80 compared to EVA 40 in 48-hour incubations (Table 2). The EVA 80 also appeared to be less sensitive to sulfate concentration at this timescale, which is consistent with higher diffusivity of the sulfate into the film. However, the thermoplastic properties of EVA diminish as the percent acetate increases, leading to a tradeoff with film integrity and sample purity. Therefore, EVA40 was selected as the polymer of choice for an *in situ* sampler. However, it is noteworthy that the more polar EVA80 may be used to reduce detection limits in field applications where appropriate.

Table 2: Recoveries of $BaSO_4$ after 48 hours of exposure from barium oxalate seeded EVA films with variable acetate contents. The standard deviation of replicates (n) is shown in brackets next to the averages for each test. The isotopic composition of the initial stock sulfate solution used in each experiment was 1.1‰ ±0.1 vs. VCDT (n=3).

SO_4 (mM)	***% purity of $BaSO_4$ extracted***	***Yield (mmoles SO_4/g coating)***	***Efficiency (% Ba converted to $BaSO_4$)***	***$\partial^{34}S$ (‰ vs. VCDT)***
Ethylene vinyl acetate (**40% acetate**)				
5 (n=3)	88.7 (3.6)	0.029 (0.012)	1.7 (0.7)	1.1 (0.2)
14 (n=3)	90.8 (2.5)	0.220 (0.026)	12.4 (1.5)	1.1 (0.1)
28 (n=4)	93.8 (6.1)	0.472 (0.329)	26.6 (18.5)	1.0 (0.1)
Ethylene vinyl acetate (**80% acetate**)				
5 (n=4)	81.9 (1.9)	0.767 (0.448)	43.2 (25.3)	1.3 (0.1)
14 (n=4)	72.8 (32.1)	0.847 (0.549)	47.7 (30.9)	1.3 (0.2)
28 (n=3)	69.0 (34.2)	1.106 (0.762)	62.3 (42.9)	1.2 (0.1)

Concentration of oxalate:

The optimum ratio of BaOx to EVA was determined by comparing both the integrity of the film and the increased capacity for SO_4^{2-} uptake per addition of BaOx. Figure 1 shows the uptake curves of a 100, 200 and 300 mM solution of BaOx in EVA. There was an appreciable increase in uptake from 0.08 g $BaSO_4$ /g film to 0.55 g $BaSO_4$ /g_{film} between the 100 mM and the 200 mM films.

Thus, increasing the BaOx to EVA mole ratio from 1.8:1.0 (100mM BaOx) to 3.5:1.0 (200mM BaOx) resulted in a more that 6 fold increase of uptake. At 300 mM BaOx (an BaOx:EVA ratio of 5.0:1.0), the organic barium overwhelmed the integrity of the film and the uptake efficiency dropped to half that of the 200 mM film, indicating no additional benefit of the added barium. It is likely that at these high concentrations the BaOx loses efficiency due to clustering of the BaOx since the film was clearly less uniform with visible patches of BaOx. The 200 mM film was therefore chosen as optimal for the *in situ* sampler. An additional uptake experiment was performed where the film consisted of a 200 mM BaOx layer protected by an outer layer of pure EVA (no BaOx) to examine effects on uptake and retention of precipitate. Figure 1 illustrates that this final treatment slowed uptake, suggesting that uptake is diffusion-limited and that loss of $BaSO_4$ from an unprotected EVA film to the environment is not a significant concern. The original coating of 200 mM BaOx was able to retain precipitated sulfate and accumulate more precipitate than the 200 mM plus pure EVA sampler even after 48 h. Based on these results, the 200mM sampler was used for further optimization without an additional protective EVA coating.

Figure 1: Sampler uptake for 100, 200, 300 mM and combined 200mM barium oxalate (2 coats) and 1 final coat of pure EVA all exposed to 28 mM solution. The uptake is expressed as g barium sulfate per gram film.

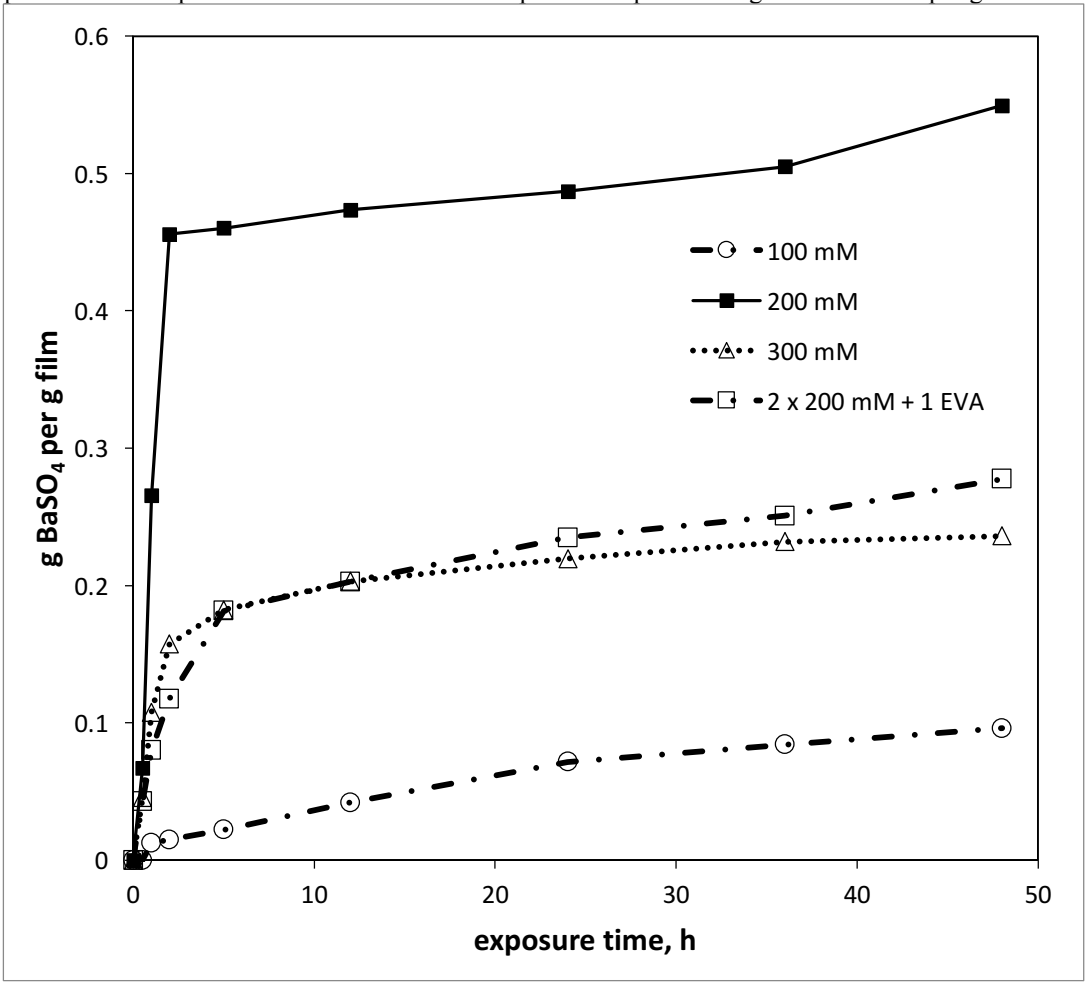

Uptake as a function of aqueous SO_4^{2-} concentration:

The 200 mM sampler was optimized for sampling times at different sulfate concentrations (Figure 2). In all cases (1 to 28 mM SO_4^{2-} solutions) less than 3% of the total dissolved sulfate was recovered in the films and therefore the ambient concentration was minimally changed. Curves showed a period of fast uptake from 0 to 2 h followed by slower uptake for the remaining period. The uptake rates are summarized in Table 4. The time for rapid uptake is proportional to ambient SO_4^{2-} concentration and ranged from 1 to 2 h for 1 to 28 mM SO_4^2. At the end of rapid uptake approximately 6 to 8% of all available barium in the film had precipitated across the 1 to 28 mM SO_4^2 treatments. At 48 h, 10 to 21% of the available barium in the film had precipitated. Sulfate

uptake into the film is also qualitatively visible as an increase in film opacity with increased exposure time (Figure S2). The average uptake rate over the first two hours was 0.0315 ± 0.004 h^{-1} or 4.5 x 10^{-4} ± 0.5 x 10^{-4} $cm^{-2}h^{-1}$. Uptake kinetics in both saline and freshwater incubations were not significantly different from each other and the effect of water temperature on uptake rates was not included in this study. A small effect of temperature on uptake rates may be expected due to slower diffusion at lower temperatures and will be investigated in a future study.

Figure 2: Uptake of the 200mM BaOx film samplers for varying ambient sulfate concentrations ranging from 1 to 28 mM sulfate.

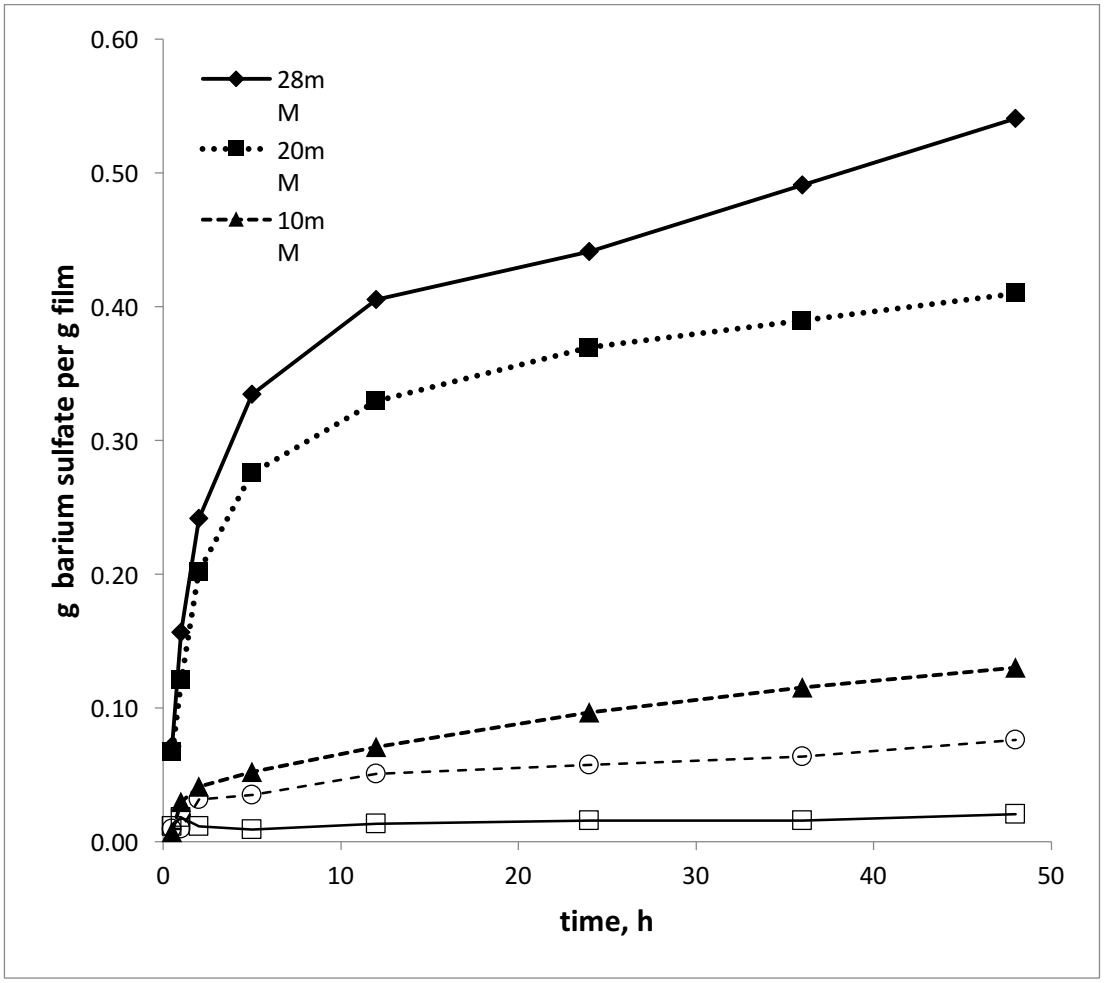

Isotopic Ratios:

The sulfur isotopic composition of the barium sulfate captured on the thin film was measured to quantify any isotopic fractionation between the media and the sampler during either diffusion or

exchange within the film. The stock solution of Na_2SO_4 used in the laboratory experiments had an isotopic ratio of 1.1‰ ± 0.1. The effect of variable acetate content of the EVA was negligible and sulfate captured by the film after 48 hours was identical to the sulfate in solution within error (Table 2). The effect of sulfate concentration after 48 hours of exposure yielded a slight positive relationship between $\partial^{34}S$ and % of barium converted (corresponding to the sulfate concentration in the environment) (Table 3). The isotope offset between aqueous sulfate and that sulfate captured on the film increased by 0.5‰ as aqueous sulfate concentration increased from 2 to 28 mM. The final film design had a very high efficiency (as % barium converted to $BaSO_4$) when sulfate concentrations were high (>20 mM) and exposure time was long (48 hours). It was also apparent that film efficiency decreased rapidly as sulfate concentrations decreased, reaching an effective 33% efficiency of barium conversion below 10 mM sulfate that was also associated with a slight isotopic fractionation (Table 3). For most environmental applications, a 48-hour exposure time is too long to capture critical *in situ* processes (e.g., diel cycling). Additional testing over a range of exposure times revealed a linear increase in $BaSO_4$ yield over the first 48 hours but a constant $\partial^{34}S$ of captured sulfate within error after 1 hour of exposure that was offset from the solution by ~0.5‰ (Table 3). Despite the relatively high variability in purity and yield of $BaSO_4$, due to remaining imperfections in extraction procedure and spatial heterogeneities in the films, the film design described herein captures an isotopically representative sulfate sample from aqueous environments.

A final test was conducted by exposing thin films to a synthetic chemical gradient of both sulfate concentration and isotopic composition. The isotopic composition of sulfate captured by the film agreed closely with the porewater composition (Figure 3a). The yield of sulfate captured by the film corresponds somewhat non-linearly to the sulfate concentration in porewaters (Figure

3b), though the discrepancy does not interfere with the fidelity of the film to record $\partial^{34}S$ of sulfate in solution, even in sediments. Further work optimizing the extraction protocol and film homogeneity should increase the fidelity of the captured sulfate to aqueous sulfate concentrations though this needs to be calibrated in various sediment matrices.

Table 3: Recoveries of $BaSO_4$ from the final thin film design (200 mM barium oxalate in 40% acetate EVA) for two experiments: (1) exposed to variable sulfate concentrations for 48 hours (n=3), and (2) exposed to 28 mM sulfate over a timeseries (n=2). The standard deviation of replicates is shown in brackets next to the averages for each test. The isotopic composition of the initial stock sulfate solution used in the 48 hour exposure experiment was 1.1‰ ±0.1 vs. VCDT (n=3); the initial stock solution used in the 28 mM exposure was -6.4‰± 0.2 vs. VCDT (n=3).

	% purity of $BaSO_4$ extracted	***Yield (mmoles SO_4/g coating)***	***Efficiency (% Ba converted to $BaSO_4$)***	***$\partial^{34}S$‰ (wrt VCDT)***
48 hour exposure				
2 mM SO_4	87.7 (4.5)	0.620 (0.085)	34.9 (4.8)	0.1 (0.1)
5 mM SO_4	82.9 (5.1)	0.572 (0.120)	32.2 (6.7)	0.2 (0.2)
10 mM SO_4	74.9 (11.0)	0.589 (0.089)	33.2 (5.0)	0.3 (0.1)
15 mM SO_4	100.8 (0.6)	0.979 (0.116)	55.1 (6.5)	0.3 (0.1)
20 mM SO_4	83.4 (3.8)	1.600 (0.156)	90.1 (8.8)	0.6 (0.1)
28 mM SO_4	89.9 (7.7)	1.727 (0.056)	97.3 (3.1)	0.5 (0.1)
28 mM SO_4 exposure				
0.5 hr	7.4 (6.0)	0.034 (0.016)	1.9 (0.9)	-5.2 (0.3)
1 hr	23.6 (21.2)	0.061 (0.025)	3.4 (1.4)	-5.9 (0.2)
4 hr	49.0 (53.9)	0.132 (0.009)	7.4 (0.5)	-5.7 (0.4)
6 hr	54.5 (45.3)	0.187 (0.101)	10.5 (5.7)	-5.8 (0.2)
24 hr	82.2 (1.5)	0.573 (0.035)	32.3 (2.0)	-5.9 (0.2)
48 hr	57.8 (25.3)	0.816 (0.566)	45.9 (31.9)	-5.8 (0.2)
168 hr	93.5 (8.8)	0.977 (0.258)	55.0 (14.5)	-5.9 (0.1)

Figure 3: Thin films were exposed to an artificial chemical gradient (both sulfate concentration and isotopic composition) in sediment porewaters for 7.5 hours. The chemocline was established with increasing $\partial^{34}S$ as concentration of sulfate decreased (a) The isotopic composition of the sulfate captured and extracted from the thin film (dashed line) agrees closely with the porewater sulfate (solid line). (b) The yield of sulfate captured by the film generally tracks with the sulfate concentration gradient in water though film uptake is enhanced at the higher concentrations.

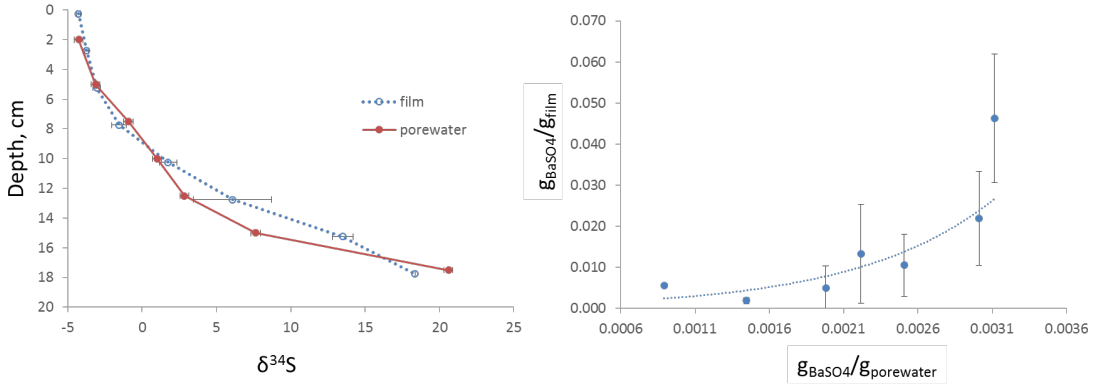

High-resolution characterization of BaOx film:

Given the incomplete conversion of the available barium oxalate (Table 2), the spatial distribution of barium oxalate and barium sulfate within the film was investigated further using high-resolution imaging and analysis by SEM-EDS. The surface of thin film exposed for 6 hours to sulfate-free water is relatively uniform on the millimeter scale, although on smaller scales more relevant to SIMS analyses (< 100 μm) the coating has fairly rough topography and a patchy distribution of BaOx (Figure S3a). The elemental composition of the sulfate-free film reflects the dominance of EVA in the analysis until the area becomes small enough to resolve the BaOx in the signal (Table 5). Small, crystalline barium oxalate (2x15 μm and smaller) is imbedded in the EVA with uniform distribution (Figure S3a-c). However, large (20-50 μm diameter) clumps of BaOx are present that have a patchy distribution within the film (Figure S3a,b). The large clumps of BaOx appear to be the initial sites of conversion to $BaSO_4$ (Table 4; Figure S3b). To determine whether the BaOx clumps were distributed throughout the thickness of the film or just near the surface, a thin film was peeled off the copper substrate and mounted for SEM-EDS analysis. Although the EVA film is elastic, small tears during sample preparation allowed for a serendipitous evaluation of the interior of the film (Figure S3c). Barium sulfate is detectably present as amorphous clumps of varying sizes that easily disaggregate (Figure 4). Further investigation of the distribution and spatial relationship between the BaOx and barium sulfate using SEM-EDS indicates distinct populations in a ternary diagram of Ba, O, and S (Figure 5a). The surface topography of the area analyzed contained two adjacent clumps (Figure 5b). The cumulative scans of pixels comprising the low-S population (Phase 1 on the ternary: BaOx) and the high-S population (Phase 2 on the ternary: barium sulfate) are shown in Figure 5c. The location of Phase 1 pixels (BaOx in blue) and Phase 2 pixels ($BaSO_4$ in red) is shown in the false color image in Figure 5d and indicates fairly

uniform coverage of barium everywhere on the surface of the film. However, the distribution of barium sulfate appears to be focused at the BaOx clumps.

Table 4: Summary of SO_4^{2-} uptake rates on 70 cm^2 samplers at different ambient SO_4^{2-} concentrations. Uptake on film is expressed as fast (initial) and slow (secondary).

mM SO_4^{2-}	Uptake (2h), $mmol_{BaSO4}/g_{film}$	Uptake (48h), $mmol_{BaSO4}/g_{film}$	Fast $k_{uptake,}$ $cm^{-2}h^{-1}$ (0-2 h)	Slow $k_{uptake,,}$ $cm^{-2}h^{-1}$ (6-48h)
1	0.05	0.08	5.2×10^{-3}	5.4×10^{-4}
5	0.07	0.21	4.5×10^{-3}	3.2×10^{-4}
10	0.10	0.31	4.2×10^{-3}	3.2×10^{-4}
20	0.30	0.60	5.4×10^{-3}	1.2×10^{-5}
28	0.36	0.79	4.4×10^{-3}	1.4×10^{-5}

Table 5: Results of SEM-EDS analysis of areas on films exposed for 6 hours to sulfate-free water and 28mM sulfate solutions. Locations within each sample correspond to locations marked on SEM images in Figure S3. The balance of wt% consists of copper, which in most locations was <1%. The relative composition (wt%) was used to identify the matrix level compounds in each location and are listed in order of relative abundance.

Sample	*Location within sample*	*Area (μm^2)*	*C (wt%)*	*O (wt%)*	*S (wt%)*	*Ba (wt%)*	*Matrix-level compounds*
6hr exposure – 0mM SO_4							
control	bulk	$3.06 * 10^6$	63.5	14.7	0	17.3	EVA/BaOx
	bulk (zoom)	$1.56 * 10^4$	66.7	11.7	0	18.3	EVA/BaOx
	ROI - 1	243	63.1	11.2	0	24.9	EVA/BaOx
	ROI - 2	69	42.6	14.9	0	41.2	BaOx/EVA
6hr exposure – 28mM SO_4							
Top surface 3 clumps	bulk	$9.0 * 10^4$	61.9	14.2	0.4	23.4	EVA/BaOx
	ROI – 1	Spot	15.8	5.5	0.2	78.5	BaOx
	ROI – 2	1256	56.8	15.4	2.1	25.7	EVA/BaOx/$BaSO_4$
	ROI – 3	78	35.0	18.0	0.2	46.8	BaOx/EVA
	bulk (zoom)	3600	55.9	13.3	2.4	27.1	EVA/BaOx/$BaSO_4$
	ROI – 1	44	19.4	16.3	9.2	52.8	$BaSO_4$/BaOx
	ROI - 2	5	34.9	25.7	6.4	31.9	EVA/BaOx/$BaSO_4$
Bottom surface torn	ROI – 1	$3.9 * 10^4$	47.2	17.6	0.5	33.8	EVA/BaOx
	ROI – 2	$2.8 * 10^4$	54.5	16.4	0.7	27.4	EVA/BaOx
	ROI – 3	Spot	14.6	17.2	9.2	58.1	$BaSO_4$/BaOx
	ROI – 4	764	11.3	18.8	9.3	59.2	$BaSO_4$/BaOx
	ROI - 5	764	20.3	23.5	5.7	49.7	$BaSO_4$/BaOx
	ROI - 6	6910	15.3	22.6	9.4	51.7	$BaSO_4$/BaOx
	ROI - 7	3058	83.1	16.4	0.1	0.4	EVA

The distribution of sulfate within the thin film was investigated further using a combined SIMS-SEM approach to confirm (1) whether free sulfate (not captured as barium sulfate) was present, and (2) the relative abundance of sulfate associated with amorphous clumps of barium compared to tiny euhedral grains of barium. Companion images of the same 100x100 μm area taken by SIMS and SEM were compared for sulfur and barium abundance. The barium signal obtained by SIMS (as mass 153.9: BaO) was corrected for the matrix effects of oxygen using the SEM results; the sulfur signal (as mass 31.97) did not require any correction (Figure S3). While the SEM creates a higher resolution element map of the surface of the material (Figure 6a), the SIMS is capable of capturing element maps while sputtering through the thickness of the material (Figure 6b). The resulting false color maps show comparable results with both techniques, where the SIMS image is a composite image of the remaining thickness of film to the copper base, while the SEM image is only a surface image. Neither image indicates any appreciable unbound sulfate (bright red) that is not associated with barium (blue). The majority of barium sulfate (purple) is found within the large (~70x70 μm) clump, although several small euhedral grains are purple (e.g., in the top left corner of the image). Cross-sections of composite SIMS images (Figure 6b) indicate the 3-dimensional nature of the barium sulfate clump compared to the smaller grains buried under the surface. The distribution of sulfate within the large clump is patchy (e.g., the mottled blue and purple color in cross-section), suggesting the large clumps are composed of aggregates of nanocrystalline BaOx. The EVA surrounds each barium oxalate grain with a smooth coating, making it difficult to determine the crystal morphology of BaOx grains in SEM (Figure 6a). A few smaller barium grains have been converted to barium sulfate (purple) in this sample after 6 hours of exposure to 28 mM sulfate, but most are still barium oxalate (blue).

Figure 4: (a, LEFT) SEM image of the underside of a torn segment of thin film exposed to 28mM sulfate for 6 hours. (b, RIGHT) Zoomed in image of a disturbed clump of barium sulfate (brighter white) spilling out of the torn

EVA. EDS analysis indicated the area outlined in red contained 17.0 wt% carbon, 21.5 wt% oxygen, 8.9 wt% sulfur, and 51.8 wt% barium.

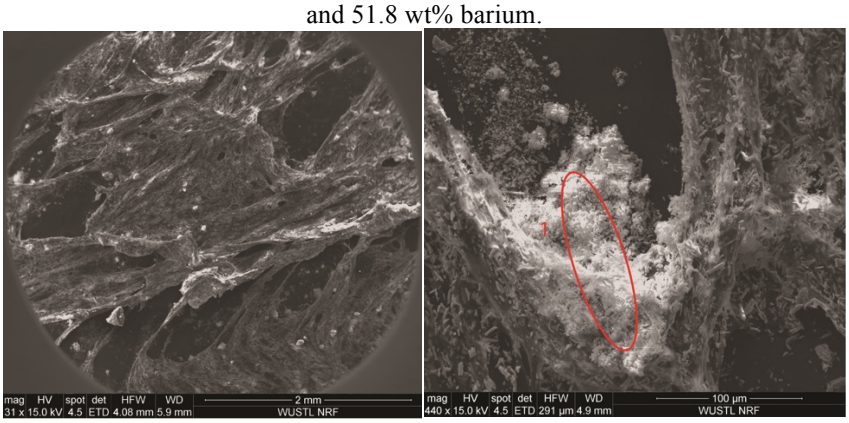

Figure 5: (a) Ternary diagram indicating the wt% Ba, wt% O, and wt% S of each pixel in the image shown in (b). (b) SEM image of the surface topography used in this analysis. Two adjacent clumps are noticeable in the bottom right quadrant of the image. (c) False color image matching that in (b) where pixels circled in (a) and labeled as Phase 1 are colored blue (e.g., barium oxalate) and pixels labeled as Phase 2 are colored red (e.g. barium sulfate). (d) Scans showing the peaks for C, O, S and Ba for the populations of pixels circled in the ternary diagram and labeled as Phase 1 (low S) and Phase 2 (high S).

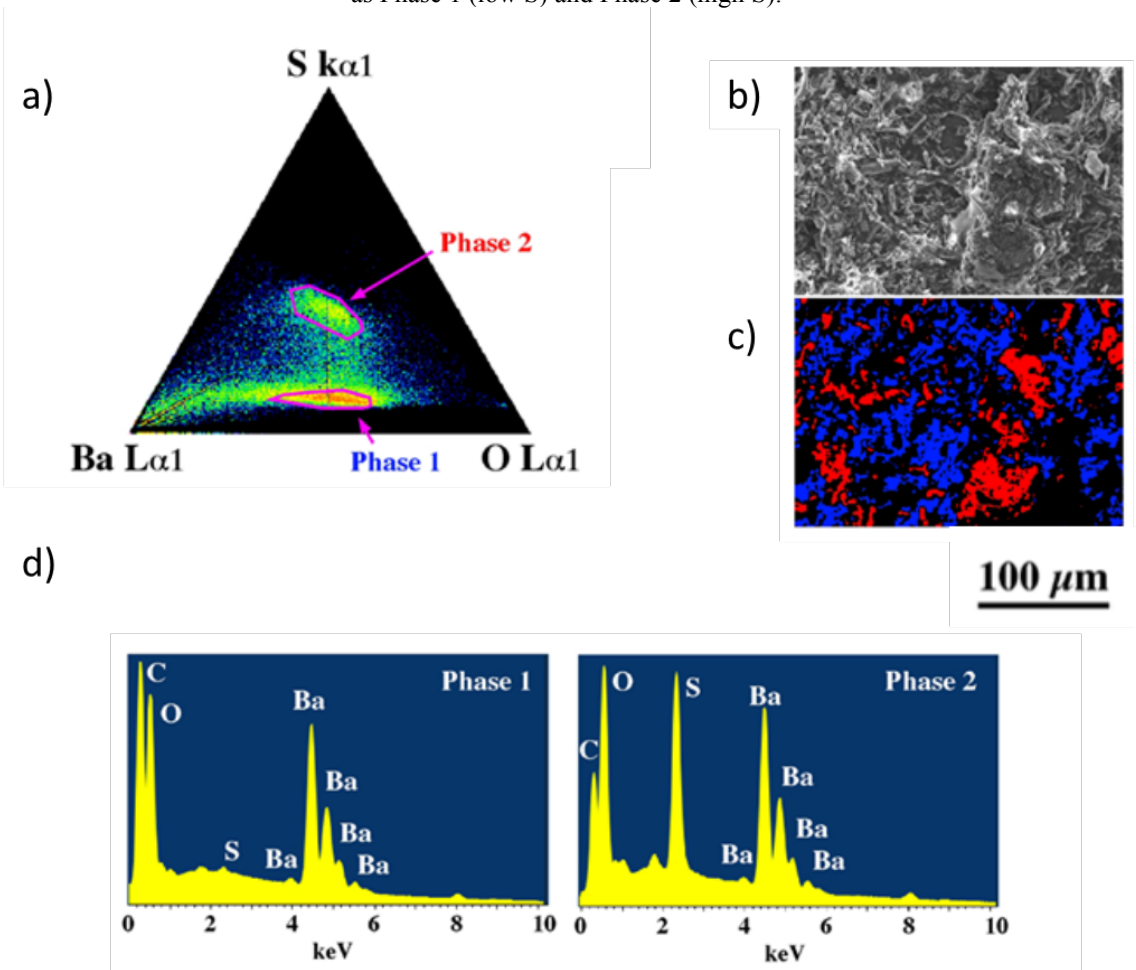

In situ analysis of the spatial distribution of sulfur within the thin film using SIMS illustrates the process of sulfate incorporation into the film as a function of concentration and exposure time. The ratio of abundance of sulfur (a trace matrix element) to the dominant matrix (sum of carbon and oxygen) provides a normalized indicator of sulfur uptake with depth into the film and allows comparison between different pieces of thin film (Figure 7). Due to the wide range in total thickness of the thin film on the 100 micron scale of the SIMS analyses, the depth profiles were normalized as a fraction of total depth by defining the base of the film (total depth of 1) as the depth at which copper ions from the underlying Cu substrate rapidly increased above background levels. Films exposed to sulfate-free water contained negligible sulfur, as expected (Figure 7). When exposed to 10mM sulfate, the film incorporated an intermediate amount of sulfur, with the greatest incorporation near the top of the thin film and a profile consistent with decreased diffusion further into the film. The overall shape of the diffusion profile and relative amount of sulfur incorporated did not significantly change with greater exposure time (Figure 7). However, the thin film with 28 mM sulfate has a profile consistent with a more constant diffusive flux with depth and with increasing relative sulfur incorporation as a function of exposure time (Figure 7). The relative abundance of barium in these films was patchy even within the depth profiles and was inconsistent from one piece to the next (Figure 8), likely due to the random distribution of larger barium oxalate clumps. However, as there is always excess barium oxalate available in the thin film (Table 3), the patchy distribution of barium in the film does not seem to impede incorporation and capture of sulfate. The SIMS concentration profiles support the bulk uptake experiment results and suggest that both the diffusion rate of sulfate into the film and the capture of sulfate by barium oxalate both vary as a function of concentration and time. The results are consistent with a model in which the diffusive flux of sulfate into the film decreases with depth and requires a large

concentration gradient to overcome the relatively slow diffusion rate through the EVA (Figure 9). In addition, given that the BaOx is present primarily in two forms (e.g., heterogeneously distributed, large, amorphous clumps and uniformly distributed, tiny, euhedral grains), the results are consistent with capture of most of the sulfate relatively rapidly by the larger barium oxalate clumps, followed by slower capture of a small additional fraction of sulfate by tiny euhedral barium oxalate (Figure 9).

Figure 6: (a) SEM image (top) and element map (bottom) showing the distribution of sulfur and barium in a film exposed to 28 mM sulfate for 6 hours. (b) Corrected false color image of sulfur (red) and barium (blue) from the SIMS.

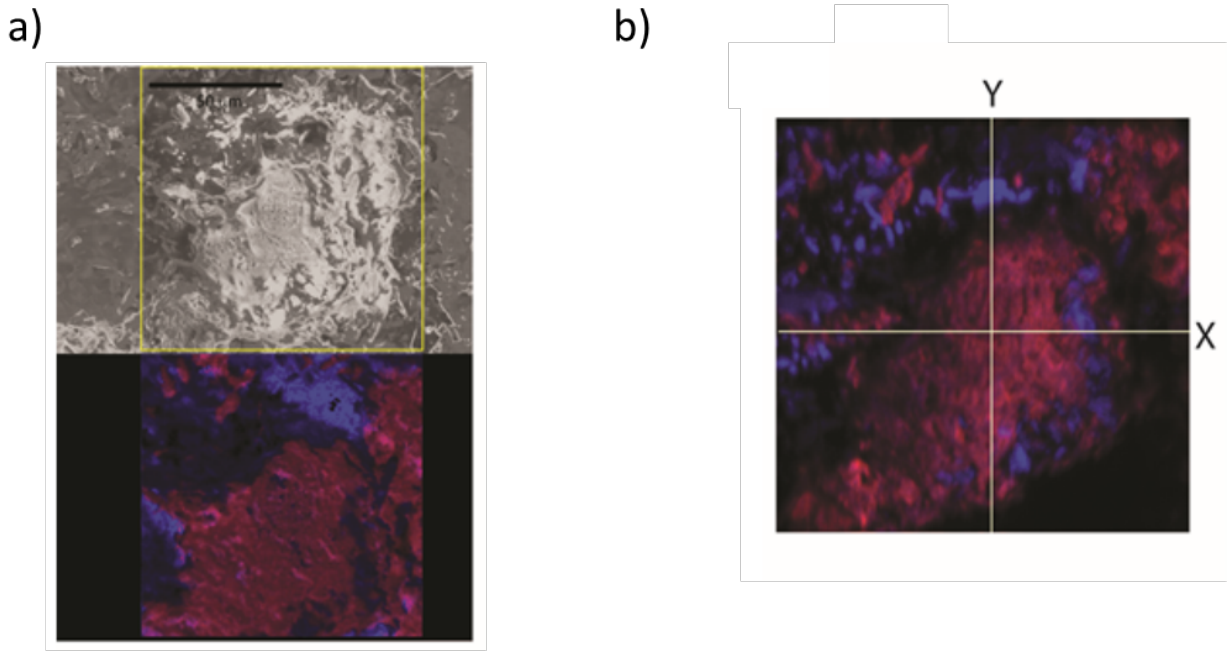

Figure 7: Average SIMS depth profiles of sulfur abundance taken from 8-10 randomly selected spots on films exposed to 0 mM, 10 mM, and 28 mM sulfate solutions (in DI water) for (a) 2 hours and (b) 6 hours. Depth has been normalized to total thin film thickness of each individual profile. Sulfur abundance is reported as a ratio of sulfur counts to the sum of carbon and oxygen counts to allow direct comparison between locations regardless of changes in matrix.

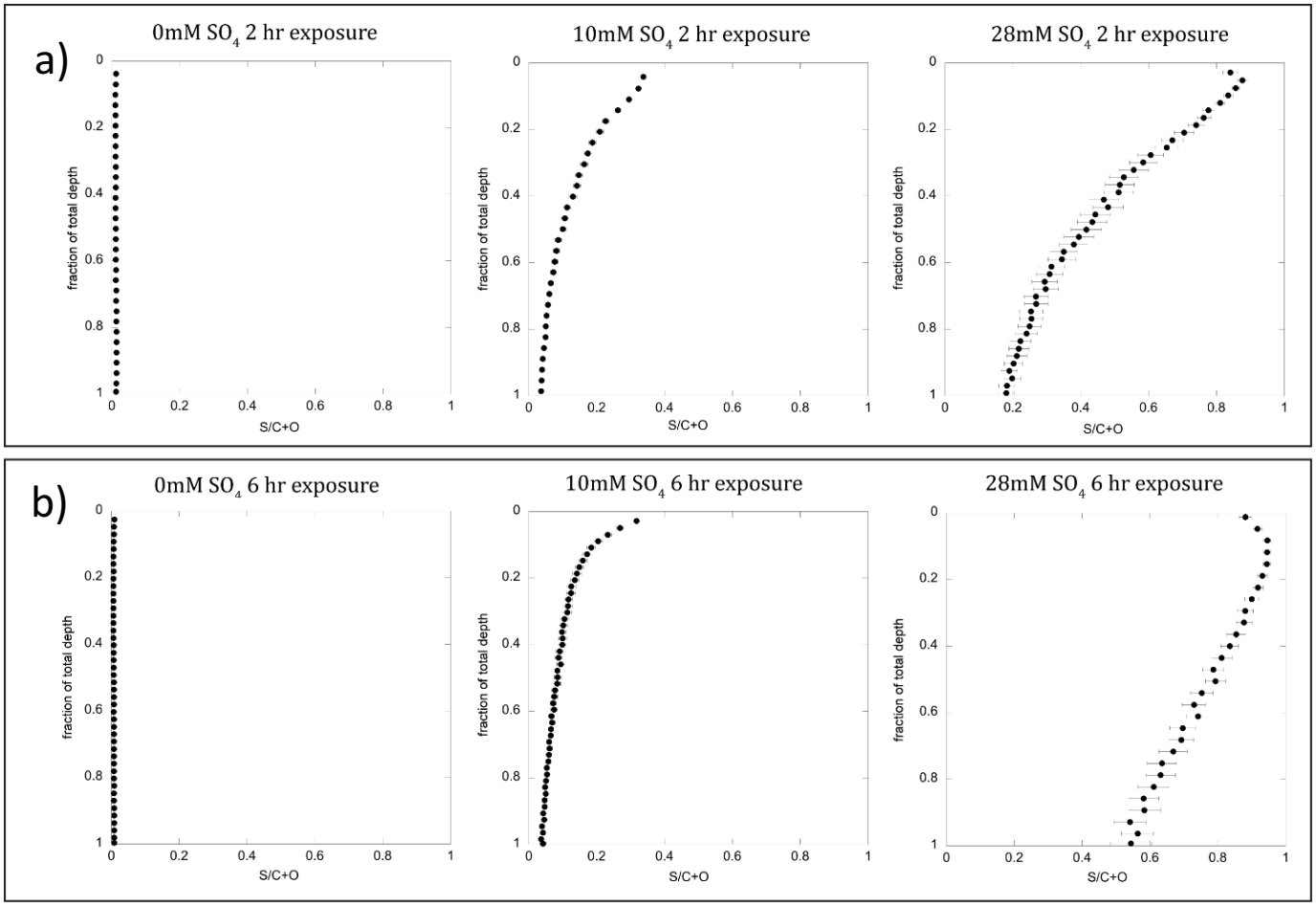

Figure 8: Average SIMS depth profiles of barium abundance that correspond to the same profiles in Figure 6 for a) 2 hr exposures and b) 6 h exposures.

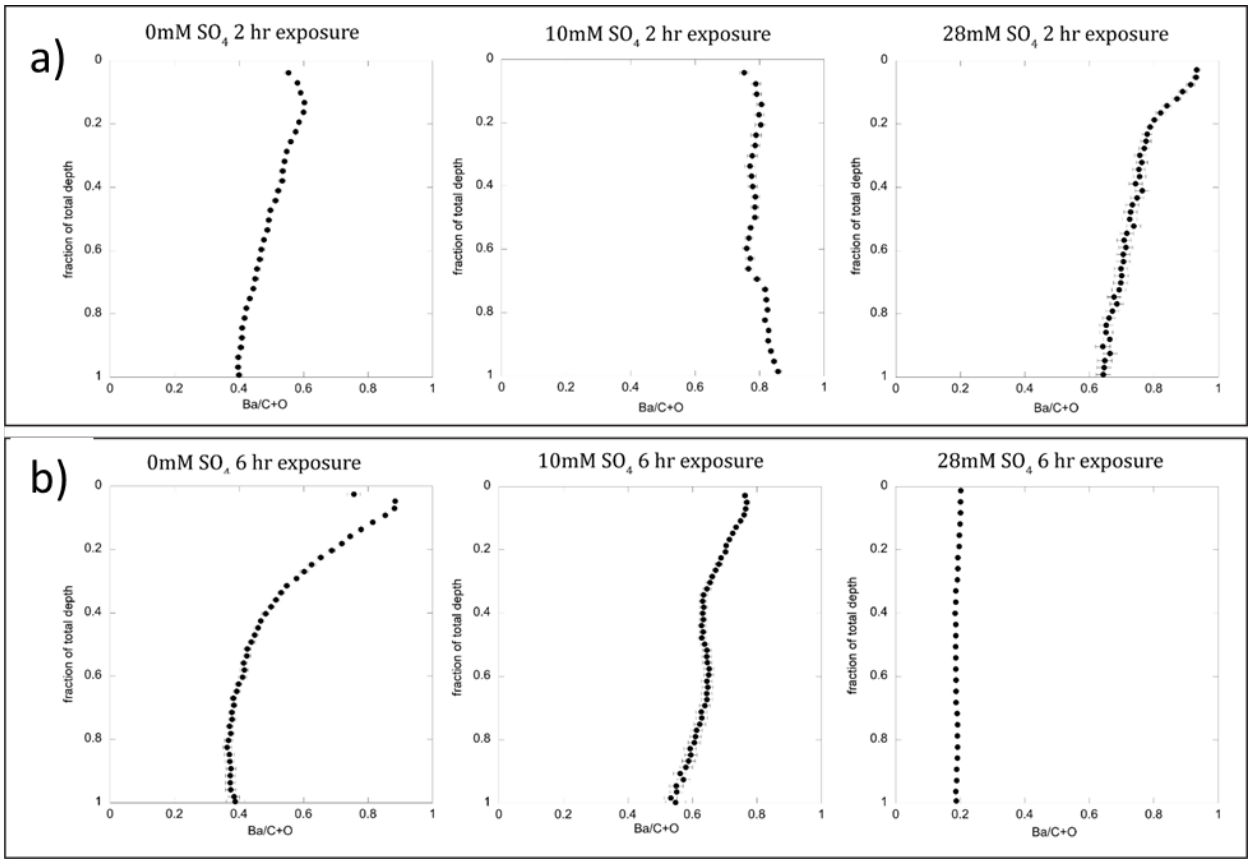

Figure 9: Schematic of a model explaining observed uptake rates and barium sulfate distribution within the thin film. The assumptions here are that (1) the heterogeneous distribution of large barium clumps is still random with respect to depth as indicated by the distribution of initial barium oxalate (black circles) and (2) that the sulfate capture rate is constant with depth and is faster by clumps than by tiny euhedral grains. The relative rates of diffusion and capture are indicated by the size of the arrows in the schematic. (a) At low sulfate concentrations (10 mM), the uptake rate data (from Figure 2) indicates a fast initial uptake rate that abruptly decreases around 2 hours and further decreases around 12 hours as drawn on the right. The companion depth profiles of sulfur abundance (from Figure 6) also indicate rapid uptake after 2 hours that does not increase appreciably even after 6 hours of exposure. The shape of the depth profiles indicate uptake is limited by diffusion at these low concentrations and is schematically illustrated with the distribution of red circles showing most of the sulfate capture takes place close to the surface of the thin film when the environment is diffusion-limited. (b) At high sulfate concentrations (28 mM), the uptake rate is still initially very fast in the first 2 hours, decreasing exponentially until 12 hours, after which the uptake rate is linear, as drawn on the right. The companion depth profile at 2 hours mirrors this faster uptake of sulfur that still retains a curvature consistent with decreasing diffusivity of sulfate with depth into the thin film. However, by 6 hours, the top of the film is saturated (indicated by the vertical segment) and deeper in the film, the

profile is a linear diffusion profile, indicating the exchange/precipitation reaction (barium sulfate for barium oxalate) is now the limiting rate rather than diffusion.

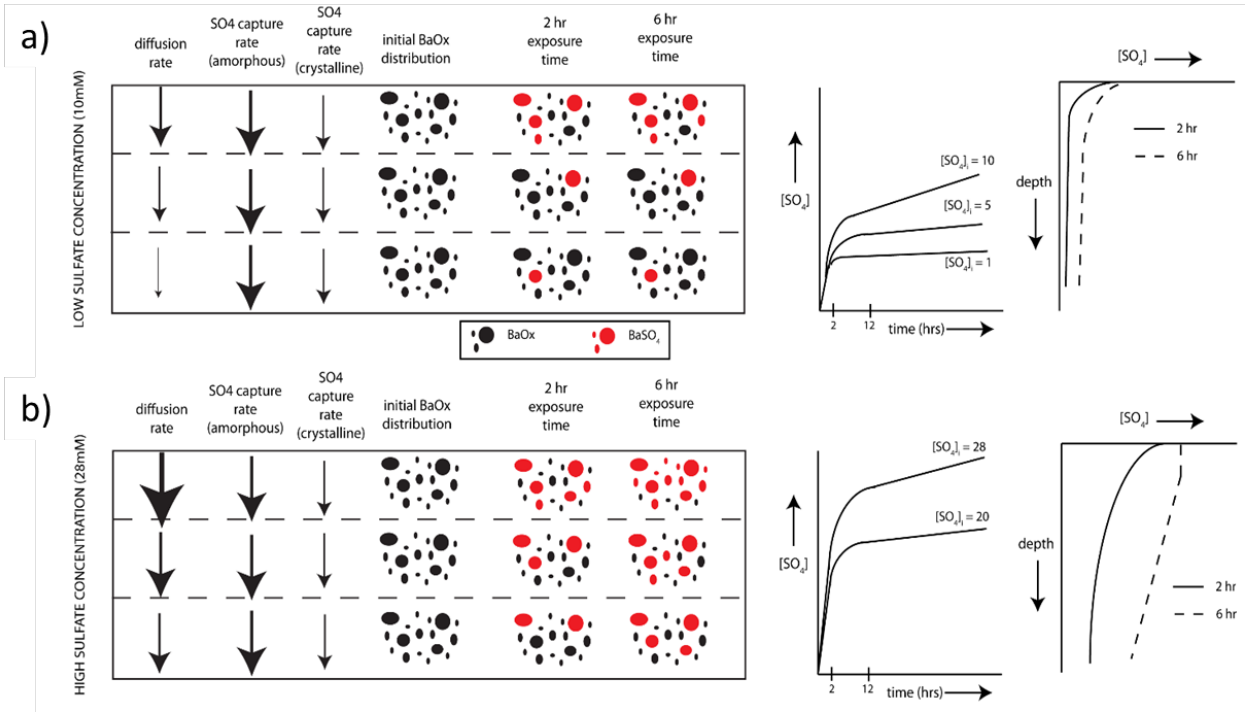

Acknowledgements

The authors would like to acknowledge support by the Gordon and Betty Moore Foundation through Grant GBMF3306 to the California Institute of Technology and NSF/EAR (#1229370) and DOE/BER (DE-SC0014613) awards to D.A.F. At Washington University in St. Louis, we also thank Stephanie Moore for assistance in processing samples, the Nano Research Facility, School of Engineering and Applied Science for assistance in acquiring SEM images; Tyrone Daulton and the Institute for Materials Science and Engineering, Washington University in St. Louis for assistance and expertise in acquiring SEM-EDS data; and Clive Jones for expertise in acquiring SIMS data. We would also like to thank Jessica Hinckley, UCONN undergraduate researcher, for sample processing and extraction.

References

1. Fike, D.A., Bradley, A.S., Rose, C.V., Rethinking the Ancient Sulfur Cycle. Annu. Rev. Earth Planet. Sci., 2015. 43: 20.1 - 20.30.
2. Jørgensen, B.B., Mineralization of organic matter in the sea bed-the role of sulphate reduction. Nature, 1982. 296: 643 - 645.
3. Fike, D.A., Gammon, C.L., Ziebis, W., Orphan, V.J., Micron-scale mapping of sulfur cycling across the oxycline of a cyanobacterial mat: a paired nanoSIMS and CARD-FISH approach. ISME Journal, 2008. 2: 749 - 759.
4. Fike, D.A., Finke, N., Zha, J., Blake, G., Hoehler, T.M., Orphan, V.J., The effect of sulfate concentration on (sub) millimeter-scale sulfide δ34S in hypersaline cyanobacterial mats over the diel cycle. Geochim. Cosmochim. Acta, 2009. 73: 6187 - 6204.
5. Wilbanks, E.G., Jaekel, U., Salman, V., Humphrey, P.T., Eisen, J.A., Facciotti, M.T., Buckley, D.H., Zinder, S.H., Druschel, G.K., Fike, D.A., Orphan, V.J., 2014. Microscale sulfur cycling in the phototrophic pink berry consortia of the Sippewissett Salt Marsh. Environ. Microbiol., 2014. 16(11): 3398 - 3415.
6. Gilhooly, W.P., Fike, D.A., Druschel, G.K., Price, R.E., Amend, J.P., Sulfur and oxygen isotope insights into sulfur cycling in shallow-sea hydrothermal vents. Geochem. Trans., 2014. 15: 12.
7. St. George, T., Vlahos, P., Harner, T., Helm, P., Wilford, B.,2011 Characterization and Field Testing of a novel Thin-Film, Rapid Equilibrating Passive Water Sampler for Organic Contaminants. Environ. Pollut., 2011., 159(1):116-124.

8. Raub, K., Vlahos, P., Whitney, M., Comparison of marine sampling methods for organic contaminants: Passive samplers, water extractions, and live oyster deployment. J. Mar. Env. Res., 2015. 109:148–158.
9. Nielsen, A., Homogeneous nucleation in barium sulfate precipitation. Acta Chem. Scand., 1961. 15: 44.

CHAPTER 4. Summary and Future Work

Through these experiments, the EVA polymer sampler was explored as an ambient passive device for the use in measuring munitions compounds in the marine environment, and isotopic sulfate concentrations in porewater. In the munitions project, it was found that it is possible to passively sorb munitions compounds in both saline and freshwater systems, and that the sorption kinetics can be characterized over the first 24 hours of exposure in the thin film configuration. It was also found that increasing salinity gradients from 0 to 5 PSU greatly increased munition sorption, but between 5-30 PSU, the $\log K_{EVA}$ was depressed slightly and similarly across all percent acetate types, but that the effect was nonlinear. Decreasing temperature does indeed increase munition sorption across all EVA types. From testing the different types of polymer in this study, the most efficient compound at sorbing TNT and RDX was EVA80, followed by EVA40 and EVA25. This is like due to dipole interactions from the increase in the more polar acetate group in the polymer chain.

The in-situ sulfate experiments were also deemed to be successful, as it was found that it is possible to seed the EVA polymer with a barium containing organic compound for the purpose of precipitating barium sulfate. Through extraction efficiency tests and trials, it was found that barium oxalate was the most ideal barium containing organic compound for this device. The spatial resolution for in-situ isotopic measurement was constrained, however, resolution could be improved in the future.

The EVA passive sampling project has wide reaching implications for the monitoring of emerging and legacy contaminants in marine systems. It is able to be both non-specific as a preliminary exploration tool (EVA40, unseeded), or as a contaminant specific device through the addition of compounds to the polymer matrix. Future work will strive to add more contaminants that EVA can reliably concentrate to the list, and to improve spatial resolution for inorganic, isotopic measurements. Ultimately, the passive sampling device could be made into sensors for the detection of these compounds in the environment, but at the moment, improving detection for a wide range of compounds is of the utmost importance.

APPENDIX I: Combined Works Cited

Ch. 2- MUNITIONS REFERENCES

1. Ariyarathna, Thivanka, Vlahos, Penny, Tobias, Craig, Smith, Richard. "Sorption Kinetics of TNT and RDX in Anaerobic Freshwater and Marine Sediments: Batch Studies." *Environmental Toxicology and Chemistry.* 2015

2. Ballentine, Mark., Tobias, Craig., Vlahos, Penny., Smith, Richard W., Cooper, Christopher. "Bioconcentration of TNT and RDX in Coastal Marine Biota." *Archives of Environmental Contamination and Toxicology* 2014. Vol 67.

3. Drzyzga, O., Gorontzy, T., Schmidt, A., Blotevogel, K.H. "Toxicity of Explosives and Related Compounds to the Luminescent Bacterium *Vibrio fischeri* NRRL-B-11177." *Archives of Environmental Contamination and Toxicology* 1995. Vol 28: 229-235.

4. Kalderis, Dimitrios., Juhasz, Albert L., Boopathy, Raj., Comfort, Steve. "Soils contaminated with explosives: Environmental fate and evaluation of state-of-the-art remediation processes (IUPAC Technical Report)." *Pure Appl. Chem.* 2011. Vol 83: 1407-1484

5. Phillips, Carlton T., Checkai, Ronald T., Kuperman, Roman G., Simini, Michael, Kolakowski, Jan E., Kurnas, Carl W. "Environmental Toxicity of the Explosives RDX and TNT in Soil to the Soil Invertebrate *Folsomia Candida*." Internal Report, US Army Edgewood Chemical Biological Center, 2004

6. Raub, Kristen B., Vlahos, Penny, Whitney, Michael. "Comparison of marine sampling methods for organic contaminants: Passive samplers, water extractions, and live oyster deployment." Marine Environmental Research, 2015. Vol 109: 148-158

7. Smith, Richard W., Vlahos, Penny., Tobias, Craig., Ballentine, Mark., Ariyarathna, Thivanka., Cooper, Christopher. "Removal Rates of Dissolved Munitions Compounds in Seawater." *Chemosphere* 2013. Vol 92: 898-904.

8. Smith, Richard W., Tobias, Craig., Vlahos, Penny., Cooper, Christopher., Ballentine, Mark., Ariyarathna, Thivanka., Fallis, Stephen., Groshens, Thomas J. "Mineralization of RDX-Derived Nitrogen

to N2 via Denitrification in Coastal Marine Sediments." *Environmental Science & Technology* 2015. Vol 49: 2180-2187.

9. St. George, Tiffany., Vlahos, Penny., Harner, Tom., Helm, Paul., Wilford, Byrony. "A rapidly equilibrating, thin film, passive water sampler for organic contaminants; Characterization and field testing." *Environmental Pollution* 2011. Vol 159: 481-486

10. Tucca, Felipe., Moya, Heriberto., Barra, Ricardo. "Ethylene vinyl acetate polymer as a tool for passive sampling monitoring of hydrophobic chemicals in the salmon farm industry." *Marine Pollution Bulletin* 2014: Vol 88: 174-179.

11. Yinon, J. "Toxicity and Metabolism of Explosives." CRC Press: Boca Raton, FL, 1990

Ch. 3- In-situ Sulfate Sampler References

1. Fike, D.A., Bradley, A.S., Rose, C.V., Rethinking the Ancient Sulfur Cycle. Annu. Rev. Earth Planet. Sci., 2015. 43: 20.1 - 20.30.
2. Jørgensen, B.B., Mineralization of organic matter in the sea bed-the role of sulphate reduction. Nature, 1982. 296: 643 - 645.
3. Fike, D.A., Gammon, C.L., Ziebis, W., Orphan, V.J., Micron-scale mapping of sulfur cycling across the oxycline of a cyanobacterial mat: a paired nanoSIMS and CARD-FISH approach. ISME Journal, 2008. 2: 749 - 759.
4. Fike, D.A., Finke, N., Zha, J., Blake, G., Hoehler, T.M., Orphan, V.J., The effect of sulfate concentration on (sub) millimeter-scale sulfide δ34S in hypersaline cyanobacterial mats over the diel cycle. Geochim. Cosmochim. Acta, 2009. 73: 6187 - 6204.

5. Wilbanks, E.G., Jaekel, U., Salman, V., Humphrey, P.T., Eisen, J.A., Facciotti, M.T., Buckley, D.H., Zinder, S.H., Druschel, G.K., Fike, D.A., Orphan, V.J., 2014. Microscale sulfur cycling in the phototrophic pink berry consortia of the Sippewissett Salt Marsh. Environ. Microbiol., 2014. 16(11): 3398 - 3415.
6. Gilhooly, W.P., Fike, D.A., Druschel, G.K., Price, R.E., Amend, J.P., Sulfur and oxygen isotope insights into sulfur cycling in shallow-sea hydrothermal vents. Geochem. Trans., 2014. 15: 12.
7. St. George, T., Vlahos, P., Harner, T., Helm, P., Wilford, B.,2011 Characterization and Field Testing of a novel Thin-Film, Rapid Equilibrating Passive Water Sampler for Organic Contaminants. Environ. Pollut., 2011., 159(1):116-124.
8. Raub, K., Vlahos, P., Whitney, M., Comparison of marine sampling methods for organic contaminants: Passive samplers, water extractions, and live oyster deployment. J. Mar. Env. Res., 2015. 109:148–158.
9. Nielsen, A., Homogeneous nucleation in barium sulfate precipitation. Acta Chem. Scand., 1961. 15: 44.